4 Silvestri G, Bertini E, Servidei S, Rana M, Zachara E, Ricci E, Tonali P: Maternally inherited cardiomyopathy: a new phenotype associated with the A to G AT nt.3243 of mitochondrial DNA (MELAS mutation). Muscle Nerve 1997;20:221–225.
5 van den Ouweland JM, Lemkes HH, Ruitenbeek W, Sandkuijl LA, de Vijlder MF, Struyvenberg PA, van de Kamp JJ, Maassen JA: Mutation in mitochondrial tRNA(Leu) (UUR) gene in a large pedigree with maternally transmitted type II diabetes mellitus and deafness. Nat Genet 1992;1:368–371.
6 Reardon W, Ross RJ, Sweeney MG, Luxon LM, Pembrey ME, Harding AE, Trembath RC: Diabetes mellitus associated with a pathogenic point mutation in mitochondrial DNA. Lancet 1992;340:1376–1379.
7 Zhang J, Yoneda M, Naruse K, Borgeld HJ, Gong JS, Obata S, Tanaka M, Yagi K: Peroxide production and apoptosis in cultured cells carrying mtDNA mutation causing encephalomyopathy. Biochem Mol Biol Int 1998;46:71–79.
8 Rusanen H, Majamaa K, Hassinen IE: Increased activities of antioxidant enzymes and decreased ATP concentration in cultured myoblasts with the 3243A–>G mutation in mitochondrial DNA. Biochim Biophys Acta 2000;1500:10–16.
9 Pang CY, Lee HC, Wei YH: Enhanced oxidative damage in human cells harboring A3243G mutation of mitochondrial DNA: implication of oxidative stress in the pathogenesis of mitochondrial diabetes. Diabetes Res Clin Pract 2001;54:S45–S56.
10 Indo HP, Davidson M, Yen HC, Suenaga S, Tomita K, Nishii T, Higuchi M, Koga Y, Ozawa T, Majima HJ: Evidence of ROS generation by mitochondria in cells with impaired electron transport chain and mitochondrial DNA damage. Mitochondrion 2007;7:106–118.
11 Katayama Y, Maeda K, Iizuka T, Hayashi M, Hashizume Y, Sanada M, Kawai H, Kashiwagi A: Accumulation of oxidative stress around the stroke-like lesions of MELAS patients. Mitochondrion 2009;9:306–313.
12 Ikawa M, Okazawa H, Arakawa K, Kudo T, Kimura H, Fujibayashi Y, Kuriyama M, Yoneda M: PET imaging of redox and energy states in stroke-like episodes of MELAS. Mitochondrion 2009;9:144–148.
13 Ishikawa K, Kimura S, Kobayashi A, Sato T, Matsumoto H, Ujiie Y, Nakazato K, Mitsugi M, Maruyama Y: Increased reactive oxygen species and anti-oxidative response in mitochondrial cardiomyopathy. Circ J 2005;69:617–620.
14 Cesarone MR, Belcaro G, Carratelli M, Cornelli U, De Sanctis MT, Incandela L, Barsotti A, Terranova R, Nicolaides A: A simple test to monitor oxidative stress. Int Angiol 1999;18:127–130.
15 Benzie IF, Strain JJ: The ferric reducing ability of plasma (FRAP) as a measure of 'antioxidant power': the FRAP assay. Anal Biochem 1996;239:70–76.
16 Gerardi G, Usberti M, Martini G, Albertini A, Sugherini L, Pompella A, Di LD: Plasma total antioxidant capacity in hemodialyzed patients and its relationships to other biomarkers of oxidative stress and lipid peroxidation. Clin Chem Lab Med 2002;40:104–110.
17 Dohi K, Satoh K, Ohtaki H, Shioda S, Miyake Y, Shindo M, Aruga T: Elevated plasma levels of bilirubin in patients with neurotrauma reflect its pathophysiological role in free radical scavenging. In Vivo 2005;19:855–860.
18 Yamanaka G, Kawashima H, Suganami Y, Watanabe C, Watanabe Y, Miyajima T, Takekuma K, Oguchi S, Hoshika A: Diagnostic and predictive value of CSF d-ROM level in influenza virus-associated encephalopathy. J Neurol Sci 2006;243:71–75.
19 Braekke K, Bechensteen AG, Halvorsen BL, Blomhoff R, Haaland K, Staff AC: Oxidative stress markers and antioxidant status after oral iron supplementation to very low birth weight infants. J Pediatr 2007;151:23–28.
20 Nakayama K, Terawaki H, Nakayama M, Iwabuchi M, Sato T, Ito S: Reduction of serum antioxidative capacity during hemodialysis. Clin Exp Nephrol 2007;11:218–224.
21 Kakita H, Hussein MH, Yamada Y, Henmi H, Kato S, Kobayashi S, Ito T, Kato I, Fukuda S, Suzuki S, Togari H: High postnatal oxidative stress in neonatal cystic periventricular leukomalacia. Brain Dev 2009;31:641–648.
22 Nishikawa T, Okamoto Y, Kodama Y, Tanabe T, Shinkoda Y, Kawano Y: Serum derivative of reactive oxygen metabolites (d-ROMs) in pediatric hemato-oncological patients with neutropenic fever. Pediatr Blood Cancer 2010;55:91–94.
23 Esposito LA, Melov S, Panov A, Cottrell BA, Wallace DC: Mitochondrial disease in mouse results in increased oxidative stress. Proc Natl Acad Sci USA 1999;96:4820–4825.
24 Buettner GR: Spin trapping: ESR parameters of spin adducts. Free Radic Biol Med 1987;3:259–303.
25 Alberti A, Bolognini L, Macciantelli D, Carratelli M: The radical cation of N,N-diethyl-para-phenylendiamine: a possible indicator of oxidative stress in biological samples. Res Chem Intermed 2000;26:253–267.

Journal of Human Genetics (2012) 57, 772–775

www.nature.com/jhg

ORIGINAL ARTICLE

Extended screening for major mitochondrial DNA point mutations in patients with hereditary hearing loss

Tomofumi Kato[1,2], Yutaka Nishigaki[2], Yoshihiro Noguchi[3], Noriyuki Fuku[2], Taku Ito[3], Eri Mikami[2], Ken Kitamura[3] and Masashi Tanaka[2]

Hearing loss (HL) is the most common sensory disorder in humans. Many patients with mitochondrial diseases have sensorineural HL (SNHL). The HL of these patients manifests as a consequence of either syndromic or nonsyndromic mitochondrial diseases. Furthermore, the phenotypes vary among patients even if they are carrying the same mutation. Therefore, these features make it necessary to analyze every presumed mutation in patients with hereditary HL, but the extensive analysis of various mutations is laborious. We analyzed 373 patients with suspected hereditary HL by using an extended suspension-array screening system for major mitochondrial DNA (mtDNA) mutations, which can detect 32 other mtDNA mutations in addition to the previously analyzed 29 mutations. In the present study, we detected 2 different mtDNA mutations among these 373 patients; m.7444G>A in the *MT-CO1* gene and m.7472insC in the *MT-TS1* gene in 1 patient (0.3%) for each. As these two patients had no clinical features other than HL, they had not been suspected of having mtDNA mutations. This extended screening system together with the previous one is useful for the genetic diagnosis and epidemiological study of both syndromic and nonsyndromic HL.
Journal of Human Genetics (2012) **57**, 772–775; doi:10.1038/jhg.2012.109; published online 13 September 2012

Keywords: hereditary hearing loss; mitochondrial DNA; mutation; suspension array

INTRODUCTION

We can find many patients with hearing loss (HL) among those with mitochondrial DNA (mtDNA) mutations. These patients are classified into two categories; those having only HL (nonsyndromic HL) and those with HL plus other symptoms of mitochondrial disease (syndromic HL). Furthermore, as the severities and phenotypes of mitochondrial diseases vary from patient to patient, we often find mtDNA mutations in unexpected cases.[1] The fact that there are many cases without any apparent family history makes it more difficult to diagnose mitochondrial diseases.[2] Sensorineural HL (SNHL) is the most common sensory disorder in humans, having a prevalence of 2.7 per 1000 in children under 5 years of age.[3] The frequency of patients with HL caused by mtDNA mutations increases with age, because mitochondrial diseases usually become aggravated with age. Therefore, it is necessary to analyze many different suspected mutations in mtDNA, but it is very exhaustive to examine these muations one by one.

Previously, we reported the results of extensive and rapid screening for major 29 major point mutations of mtDNA in patients with hereditary HL by using a suspension array technology.[4] Our previous survey of 373 patients with suspected HL by use of this screening system revealed the m.1555A>G mutation in 11 patients, the m.3243A>G mutation in 9 patients, and the m.8348A>G, m.11778G>A and m.15498G>A mutations in 1 patient each. In the present extended study, we increased the number of mutations that could be detected from 29 to 61. We examined the applicability of this extended screening system for genetic diagnosis of hereditary HL by analyzing these same 373 patients with suspected hereditary HL.

MATERIALS AND METHODS

Patients

The study population included 373 unrelated Japanese patients with suspected hereditary HL, who visited the outpatient clinic of the Department of Otolaryngology, University Hospital of Medicine, Tokyo Medical and Dental University. The subjects included patients with a family history of HL and those with no apparent cause of HL, even though they did not have any apparent family history of HL. Their detailed demographic and audiometric features are shown in Table 1. The average age of them was 40 years, with a range between 1 and 77 years.

The study protocol complied with the Declaration of Helsinki, and it was also approved by the Committee on the Ethics of Human Research of the Tokyo Metropolitan Institute of Gerontology and the Institutional Review Board (IRB no. 68) of Tokyo Medical and Dental University. This study was carried out only after obtaining the written informed consent of each individual and/or the parents in the case of children.

[1]Department of Otolaryngology, Tokyo Metropolitan Geriatric Hospital and Institute of Gerontology, Tokyo, Japan; [2]Department of Genomics for Longevity and Health, Tokyo Metropolitan Institute of Gerontology, Tokyo, Japan and [3]Department of Otolaryngology, Tokyo Medical and Dental University, Tokyo, Japan
Correspondence: Dr M Tanaka, Department of Genomics for Longevity and Health, Tokyo Metropolitan Institute of Gerontology, 35-2 Sakae-cho, Itabashi-ku, Tokyo 173-0015, Japan.
E-mail: mtanaka@tmig.or.jp
Received 27 June 2012; revised 14 August 2012; accepted 15 August 2012; published online 13 September 2012

Table 1 Demographic features of HL patients

Sex	
Male (%)	144 (38.6)
Female (%)	229 (61.4)
Onset age of HL (years)	
Newborn or 0 (%)	31 (8.3)
1~3 (%)	23 (6.2)
4~10 (%)	80 (21.4)
11~20 (%)	43 (11.5)
21~30 (%)	39 (10.5)
31~40 (%)	50 (13.4)
41~50 (%)	37 (9.9)
51~60 (%)	31 (8.3)
61~70 (%)	12 (3.2)
71~80 (%)	5 (1.3)
Unknown (%)	22 (5.9)
Mode of inheritance	
Autosomal dominant (%)	92 (24.7)
Autosomal recessive (%)	52 (13.9)
Maternal (%)	47 (12.6)
X-linked (%)	0
Sporadic (%)	179 (48.0)
Unknown (%)	3 (0.8)
Type of audiogram	
High-frequency steeply sloping (%)	80 (21.4)
High-frequency gently sloping (%)	104 (27.9)
Flat (%)	39 (10.5)
U-shaped (Cookiebite) (%)	39 (10.5)
Reverse U-shaped (%)	4 (1.1)
Low frequency (%)	39 (10.5)
Deafness (%)	21 (5.6)
Others (%)	43 (11.5)
Unknown (%)	4 (1.1)
Total (%)	373 (100)

Abbreviation: HL, hearing loss.

Extended screening of mtDNA pathological mutation by use of suspension-array technology

DNA samples were purified from the blood by using a standard procedure. The mtDNA from each patient was analyzed with the previously described extended suspension array-based screening system.[5] The targets of the present analysis were 32 mtDNA mutations in 15 genes: 1 in each of *MT-TQ* ($tRNA^{Gln}$), *MT-TW* ($tRNA^{Trp}$), *MT-TC* ($tRNA^{Cys}$), *MT-TH* ($tRNA^{His}$), *MT-TL2* ($tRNA^{Leu(CUN)}$), *MT-ND6* and *MT-CYB* genes; 2 in each of *MT-TN* ($tRNA^{Asn}$), *MT-ATP6*, *MT-TG* ($tRNA^{Gly}$) and *MT-TE* ($tRNA^{Glu}$) genes; 3 in the *MT-ND3* gene; 4 in the *MT-CO1* gene; and 5 in each of the *MT-TI*($tRNA^{Ile}$) and *MT-TS1* ($tRNA^{Ser(UCN)}$) genes as shown in Table 2. The mtDNA mutations reported in our previous study were within the DNA fragments amplified by multiplex PCR for mtDNA haplotyping, which was mainly designed for anthropological purposes. For the present study, we newly designed a second multiplex PCR system to analyze the 32 additional mtDNA mutations (including m.7445, which is known to cause of HL).

Comparison of results between suspension array and direct DNA sequencing

DNA sequencing was carried out by using an Applied Biosystems 3130 × l Genetic Analyzer (Applied Biosystems, Foster City, CA, USA), a BigDye Terminator v3.1 Cycle Sequencing Kit (Applied Biosystems) and Sequencher version 4.2.2 (Gene Codes, Ann Arbor, MI, USA) to compare the sequences with the revised Cambridge reference sequence,[6,7] while following the standard procedure.[8,9]

Table 2 List of 32 mutations examined by use of the extended suspension array-based system for the detection of mtDNA mutation detection system

Nucleotide position (m)	*Nucleotide change*	*Amino acid change*	*Locus*	*Clinical phenotype*
4269	A>G		MT-TI	Encephalopathy/FICP
4295	A>G		MT-TI	MHCM
4298	G>A		MT-TI	CPEO/MS
4300[a]	A>G		MT-TI	MICM
4320	C>T		MT-TI	MHCM
4332	G>A		MT-TQ	MELAS/encephalopathy
5537	A>insT		MT-TW	MILS
5698	G>A		MT-TN	CPEO/MM
5703	G>A		MT-TN	CPEO/MM
5814	T>C		MT-TC	Encephalopathy
7443[b]	A>G	Ter-G	MT-CO1	DEAF
7444[b]	G>A	Ter-K	MT-CO1	LHON/SNHL/DEAF
7445[b]	A>C	Ter-S	MT-CO1	DEAF
7445[a]	A>G	Ter-Ter	MT-CO1	SNHL
7472[b]	C>insC		MT-TS1	PEM/AMDF
7497[a]	G>A		MT-TS1	MM/exercise intolerance
7510	T>C		MT-TS1	SNHL
7511[a]	T>C		MT-TS1	SNHL
7512[a]	T>C		MT-TS1	PEM/MERRF + MELAS
8993	T>C	L>P	MT-ATP6	NARP/MILS
8993	T>G	L>R	MT-ATP6	NARP/MILS
9997	T>C		MT-TG	MHCM
10010	T>C		MT-TG	PEM
10158[a]	T>C	S>P	MT-ND3	MILS
10191	T>C	S-P	MT-ND3	ESOC/Leigh-like disease/MILS
10197[a]	G>A	A-T	MT-ND3	MILS/dystonia/stroke
12147	G>A		MT-TH	MERRF + MELAS/cerebral edema
12297	T>C		MT-TL2	Dilated cardiomyopathy
14568[b]	C>T	G-S	MT-ND6	LHON
14709[a]	T>C		MT-TE	MM + DMDF/encephalomyopathy
14710	G>A		MT-TE	Encephalomyopathy + retinopathy
15243	G>A	G>E	MT-CYB	MHCM

Abbreviations: AMDF, ataxia, myoclonus and deafness; ATP6, ATP synthase F_0 subunit 6; CO1, cytochrome *c* oxidase subunit I; CPEO, chronic progressive external ophthalmoplegia; CYB, cytochrome *b*; DEAF, maternally inherited deafness or aminoglycoside-induced deafness; DMDF, diabetes mellitus + deafness; ESOC, epilepsy, strokes, optic atrophy and cognitive decline; FICP, fatal infantile cardiomyopathy, plus a MELAS-associated cardiomyopathy; LHON, Leber hereditary optic neuropathy; MELAS, mitochondrial myopathy, encephalopathy, lactic acidosis and stroke-like episodes; MERRF, myoclonic epilepsy and ragged-red fibers; MHCM, *maternally inherited hypertrophic cardiomyopathy*; MICM *maternally inherited* cardiomyopathy; MILS, maternally inherited Leigh syndrome; MR, mental retardation; MS, multiple sclerosis; mtDNA, mitochondrial DNA; NARP, neurogenic muscle weakness, ataxia and retinitis pigmentosa; ND, NADH dehydrogenase subunit; SNHL, sensorineural hearing loss; PEM, progressive encephalomyopathy.
Abbreviations and information about mutations are annotated in the MITOMAP database.
[a]Mutation reported as both homoplasmic and heteroplasmic.
[b]Mutation reported as homoplasmic.

RESULTS AND DISCUSSION

In the present extended study, 2 of the 32 mtDNA mutations, m.7444G>A and m.7472insC, were detected by the screening system, each in 1 patient out of the 373 patients with SNHL. The median fluorescent intensities for the m.7444G>A mutation and the 7472insC mutation are displayed in scatter diagrams (Figure 1). When the median fluorescent intensity values for the wild-type signals were below the cut-off values, we regarded the mutations as homoplasmic. The m.7444G>A mutation was homoplasmic and the 7472insC mutation was heteroplasmic. On the basis of the

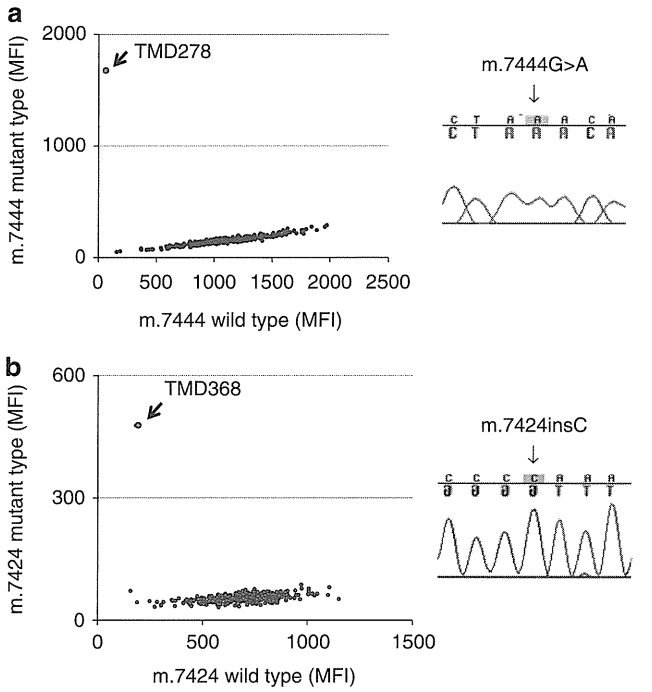

Figure 1 Scatter diagrams with mutant median fluorescent intensity values on the y axis and wild-type ones on the x axis and electropherograms of DNA sequences for the m.7444G>A homoplasmic mutation (**a**) and the m.7472insC heteroplasmic mutation (**b**). All 373 DNA samples were analyzed by the m.7444G>A and m.7472insC mutation detection systems, using universal 96-well plates. Later on, each result was merged into the two separate scatter diagrams. Red circles indicate median fluorescent intensity values for mutation-positive DNAs.

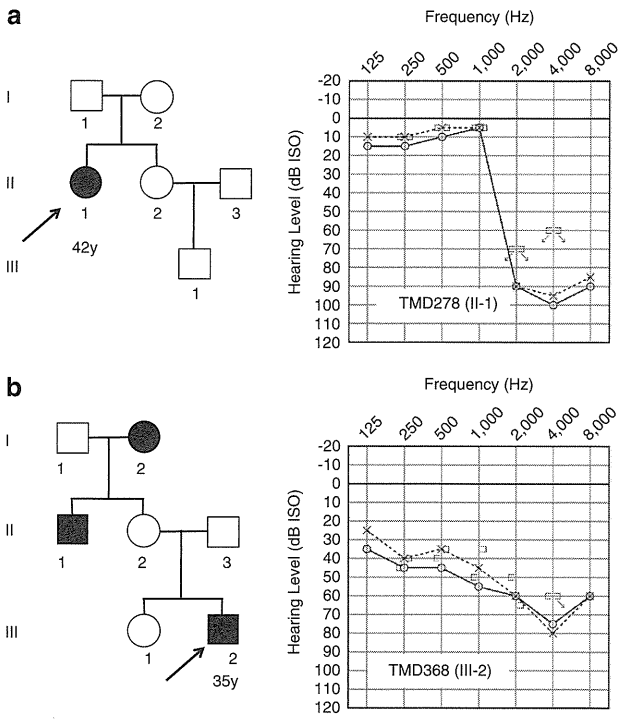

Figure 2 Pedigrees of the families and audiograms of patient TMD278 (**a**) and patient TMD368 (**b**). Clinical features are depicted: black-filled circles or squares as individuals with deafness. Arrows indicate probands. Symbols on pure tone audiograms: dB, decibels; ISO, international standards organization.], left-ear bone conduction; [, right-ear bone conduction; O, right-ear air conduction; X, left-ear air conduction.

Table 3 Mitochondrial DNA mutations detected in 373 patients with hereditary HL screened by the previous and present detection system

mtDNA mutation	*Number*	*Frequency (%)*
Previous study (Kato, 2010)		
m.1555A>G	11	2.9
m.3243A>G	9	2.4
m.8348A>G	1	0.3
m.11778G>A	1	0.3
m.15498G>A	1	0.3
Present study		
m.7444G>A	1	0.3
m.7472insC	1	0.3
Undetected	348	93.3
Total	373	100

Abbreviation: HL, hearing loss.

chromatogram, the mutation load was estimated as 59%. None of the other 30 mutations were detected in these patients with SNHL. We summarized the mtDNA mutations detected by the previous and the present analytical systems in Table 3.

SNHL is one of the most common disorder in patients with mitochondrial diseases,[10] which is represented by the mutations of the homoplasmic m.1555A>G and the heteroplasmic m.3243A>G.[11–16] We previously reported that not only these mutations but also other mutations could be detected in the patients with either nonsyndromic or syndromic hereditary HL. The m.7444G>A mutation was earlier reported as a cause of aminoglycoside-induced and nonsyndromic HL.[17] However, patient TMD278, carrying this mutation, had no history of aminoglycoside injection in her detailed clinical history. On the other hand, we should mention that this mutation characterizes haplogroup V7 and H40b, and there is no direct evidence that these haplogroups tend to have HL.[18] Furthermore, it was also reported that the m.7444G>A mutation is a secondary mutation found in patients with Leber's hereditary optic neuropathy (LHON) and that this mutation has an additional role in the pathogenesis of LHON.[19,20] Primary mutations, m.11778G>A, m.3460G>A and m.14484T>C can cause LHON. However, these mutations had already been examined in our previous study and the patient TMD278 was negative for them. With regard to her clinical data, she had high-tone SNHL as shown in Figure 2a, although she was 42 years of age. The onset of her HL occurred during her childhood, after which the HL became progressive. She had started wearing hearing aids 3 years before visiting our clinic. Her clinical feature seemed sporadic because she had neither other clinical disorders such as LHON nor a family history of HL.

The m.7472insC was reported as a pathogenic heteroplasmic mutation within the coding region of $tRNA^{Ser(UCN)}$. This mutation was previously reported to be associated with progressive myoclonus epilepsy or syndromic disorders including HL, ataxia and myoclonus in previous reports.[21] The phenotypes of this mutation, however, vary even among individuals within the same family.[22] The audiogram of TMD368 showed moderate SNHL (Figure 2b), although this patient

was still just 35 years old. He had no other clinical disorders such as myoclonus or family history of HL or neurological disorders. It should also be noted that recently the m.7472insC mutation was identified in gastric cancer tissues.[23] This report suggested that somatic mtDNA mutations may have an important role in the progression of gastric cancer.

In conclusion, the present extended screening system by use of a suspension array for major mtDNA mutations was demonstrated to be powerful, because we could detect both major causative and unexpected mtDNA mutations. The present system is helpful for both the diagnosis and epidemiological studies. Detecting mtDNA mutations in the early stage of HL could be meaningful both to select the optimal therapeutic strategies for the patients and to provide appropriate genetic counseling.

ACKNOWLEDGEMENTS

We thank Y Abe for helpful discussions and excellent technical support. This work was supported in part by grants from the programs grants-in-aid for young scientists (B)-(no. 22791577 to TK), grants-in-aid for scientific research (B)-(no. 21390459 to KK), grants-in-aid for scientific research (C) (no. 18590317 to Y Nishigaki and no. 21590411 to HH) and grants-in-aid for scientific research (A-22240072, B-21390459 and C-21590411 to MT) from the Ministry of Education Culture, Sports, Science and Technology; by a grant-in-aid for scientific research from the Ministry of Health, Labor and Welfare of Japan (H23-kankaku-005 to KK); by grants-in-aid for the Research on Intractable Diseases (Mitochondrial Disease H23-016 and H23-119) from the Ministry of Health, Labor, and Welfare (to MT); and by grants for scientific research from the Takeda Science Foundation (to MT).

1 Schapira, A. H. Mitochondrial disease. *Lancet* **368,** 70–82 (2006).
2 DiMauro, S. & Schon, E. A. Mitochondrial respiratory-chain diseases. *N. Engl. J. Med.* **348,** 2656–2668 (2003).
3 Morton, C. C. & Nance, W. E. Newborn hearing screening–a silent revolution. *N. Engl. J. Med.* **354,** 2151–2164 (2006).
4 Kato, T., Nishigaki, Y., Noguchi, Y., Ueno, H., Hosoya, H., Ito, T. *et al.* Extensive and rapid screening for major mitochondrial DNA point mutations in patients with hereditary hearing loss. *J. Hum. Genet.* **55,** 147–154 (2010).
5 Nishigaki, Y., Ueno, H., Coku, J., Koga, Y., Fujii, T., Sahashi, K. *et al.* Extensive screening system using suspension array technology to detect mitochondrial DNA point mutations. *Mitochondrion* **10,** 300–308 (2010).
6 Anderson, S., Bankier, A. T., Barrell, B. G., de Bruijn, M. H., Coulson, A. R., Drouin, J. *et al.* Sequence and organization of the human mitochondrial genome. *Nature* **290,** 457–465 (1981).
7 Andrews, R. M., Kubacka, I., Chinnery, P. F., Lightowlers, R. N., Turnbull, D. M. & Howell, N. Reanalysis and revision of the Cambridge reference sequence for human mitochondrial DNA. *Nat. Genet.* **23,** 147 (1999).
8 Nishigaki, Y., Marti, R., Copeland, W. C. & Hirano, M. Site-specific somatic mitochondrial DNA point mutations in patients with thymidine phosphorylase deficiency. *J. Clin. Invest.* **111,** 1913–1921 (2003).
9 Ueno, H., Nishigaki, Y., Kong, Q. P., Fuku, N., Kojima, S., Iwata, N. *et al.* Analysis of mitochondrial DNA variants in Japanese patients with schizophrenia. *Mitochondrion* **9,** 385–393 (2009).
10 Xing, G., Chen, Z. & Cao, X. Mitochondrial rRNA and tRNA and hearing function. *Cell Res.* **17,** 227–239 (2007).
11 Prezant, T. R., Agapian, J. V., Bohlman, M. C., Bu, X., Oztas, S., Qiu, W. Q. *et al.* Mitochondrial ribosomal RNA mutation associated with both antibiotic-induced and non-syndromic deafness. *Nat. Genet.* **4,** 289–294 (1993).
12 Noguchi, Y., Yashima, T., Ito, T., Sumi, T., Tsuzuku, T. & Kitamura, K. Audiovestibular findings in patients with mitochondrial A1555G mutation. *Laryngoscope* **114,** 344–348 (2004).
13 Goto, Y., Nonaka, I. & Horai, S. A mutation in the tRNA(Leu)(UUR) gene associated with the MELAS subgroup of mitochondrial encephalomyopathies. *Nature* **348,** 651–653 (1990).
14 Tamagawa, Y., Kitamura, K., Hagiwara, H., Ishida, T., Nishizawa, M., Saito, T. *et al.* Audiologic findings in patients with a point mutation at nucleotide 3,243 of mitochondrial DNA. *Ann. Otol. Rhinol. Laryngol.* **106,** 338–342 (1997).
15 Oshima, T., Ueda, N., Ikeda, K., Abe, K. & Takasaka, T. Hearing loss with a mitochondrial gene mutation is highly prevalent in Japan. *Laryngoscope* **109,** 334–338 (1999).
16 Vandebona, H., Mitchell, P., Manwaring, N., Griffiths, K., Gopinath, B., Wang, J. J. *et al.* Prevalence of mitochondrial 1555A–>G mutation in adults of European descent. *N. Engl. J. Med.* **360,** 642–644 (2009).
17 Zhu, Y., Qian, Y., Tang, X., Wang, J., Yang, L., Liao, Z. *et al.* Aminoglycoside-induced and non-syndromic hearing loss is associated with the G7444A mutation in the mitochondrial COI/tRNASer(UCN) genes in two Chinese families. *Biochem. Biophys. Res. Commun.* **342,** 843–850 (2006).
18 Yao, Y. G., Salas, A., Bravi, C. M. & Bandelt, H. J. A reappraisal of complete mtDNA variation in East Asian families with hearing impairment. *Hum. Genet.* **119,** 505–515 (2006).
19 Brown, M. D., Voljavec, A. S., Lott, M. T., MacDonald, I. & Wallace, D. C. Leber's hereditary optic neuropathy: a model for mitochondrial neurodegenerative diseases. *FASEB J.* **6,** 2791–2799 (1992).
20 Matsumoto, M., Hayasaka, S., Kadoi, C., Hotta, Y., Fujiki, K., Fujimaki, T. *et al.* Secondary mutations of mitochondrial DNA in Japanese patients with Leber's hereditary optic neuropathy. *Ophthalmic Genet.* **20,** 153–160 (1999).
21 Tiranti, V., Chariot, P., Carella, F., Toscano, A., Soliveri, P., Girlanda, P. *et al.* Maternally inherited hearing loss, ataxia and myoclonus associated with a novel point mutation in mitochondrial tRNASer(UCN) gene. *Hum. Mol. Genet.* **4,** 1421–1427 (1995).
22 Jaksch, M., Klopstock, T., Kurlemann, G., Dorner, M., Hofmann, S., Kleinle, S. *et al.* Progressive myoclonus epilepsy and mitochondrial myopathy associated with mutations in the tRNA(Ser(UCN)) gene. *Ann. Neurol.* **44,** 635–640 (1998).
23 Hung, W. Y., Wu, C. W., Yin, P. H., Chang, C. J., Li, A. F., Chi, C. W. *et al.* Somatic mutations in mitochondrial genome and their potential roles in the progression of human gastric cancer. *Biochim. Biophys. Acta.* **1800,** 264–270 (2010).

Mitochondrion 12 (2012) 644–653

Contents lists available at SciVerse ScienceDirect

Mitochondrion

journal homepage: www.elsevier.com/locate/mito

Metabolomic profiling rationalized pyruvate efficacy in cybrid cells harboring MELAS mitochondrial DNA mutations

Kenjiro Kami [a,b,1], Yasunori Fujita [c,1], Saori Igarashi [a], Sayaka Koike [a], Shoko Sugawara [a], Satsuki Ikeda [a], Naomi Sato [a], Masafumi Ito [c], Masashi Tanaka [d,*], Masaru Tomita [a,b,e], Tomoyoshi Soga [a,b,e]

[a] Institute for Advanced Biosciences, Keio University, Tsuruoka, Yamagata 997-0017, Japan
[b] Systems Biology Program, Graduate School of Media and Governance, Keio University, Fujisawa, Kanagawa 252-8520, Japan
[c] Research Team for Mechanism of Aging, Tokyo Metropolitan Institute of Gerontology, Itabashi, Tokyo 173-0015, Japan
[d] Department of Genomics for Longevity and Health, Tokyo Metropolitan Institute of Gerontology, Itabashi, Tokyo 173-0015, Japan
[e] Human Metabolome Technologies, Inc., Tsuruoka, Yamagata, 997-0052, Japan

ARTICLE INFO

Article history:
Received 12 June 2012
Received in revised form 21 July 2012
Accepted 30 July 2012
Available online 4 August 2012

Keywords:
MELAS
Pyruvate
Cybrid
Energy metabolism
Metabolome
CE-MS

ABSTRACT

Pyruvate treatment was found to alleviate clinical symptoms of mitochondrial myopathy, encephalopathy, lactic acidosis, and stroke-like episodes (MELAS) syndrome and is highly promising therapeutic. Using capillary electrophoresis time-of-flight mass spectrometry (CE-TOFMS), we measured time-changes of 161 intracellular and 85 medium metabolites to elucidate metabolic effects of pyruvate treatment on cybrid human 143B osteosarcoma cells harboring normal (2SA) and MELAS mutant (2SD) mitochondria. The results demonstrated dramatic and sustainable effects of pyruvate administration on the energy metabolism of 2SD cells, corroborating pyruvate as a metabolically rational treatment regimen for improving symptoms associated with MELAS and possibly other mitochondrial diseases.

1. Introduction

Mitochondrial myopathy, encephalopathy, lactic acidosis, and stroke-like episodes (MELAS) syndrome is one of the mitochondrial cytopathies first introduced by Pavlakis et al. (1984). Complex pathologies observed in MELAS patients primarily stem from the adenine-to-guanine transition mutation at position 3243 of the mitochondrial genome (A3243G) located in the mitochondrial $tRNA^{Leu(UUR\ (R=A\ or\ G))}$ gene (Goto et al., 1990), which accounts for about 80% of all cases of MELAS (Koga et al., 2012b) and is estimated to be carried by as high as 0.06% of the general population (Sproule and Kaufmann, 2008). The mutated mitochondrial $tRNA^{Leu(UUR)}$ gene recognizes the UUA but not the UUG codon and causes protein synthesis defects due to a shortened life-span of $tRNA^{Leu(UUR)}$, a lowered ratio of aminoacyl- to uncharged-$tRNA^{Leu(UUR)}$, accumulations of leucine aminoacylation and processing intermediates, and a defect in modifying uridine to 5-taurinomethyluridine at the first position of the anticodon (Koga et al., 2012b). Due to the frequent appearance of the UUG codons in the coding sequence of NADH dehydrogenase subunit 6, mitochondria in the skeletal muscle of MELAS patients often exhibit defects in activities of complex I (Ichiki et al., 1989) and complex IV and others in severe cases (Iizuka and Sakai, 2005; Yoneda et al., 1989). The defects in these respiratory complexes induce impaired oxidative phosphorylation, increased generation of free radicals, and a decreased level of free nitric oxide (Hussein et al., 2009). Disordered ATP production has also been confirmed as a pathogenesis of MELAS by studies using cytoplasmic hybrids, or "cybrids," which are human cell lines containing the patient's mitochondria with mutated genomes (DiMauro and Schon, 2003). Most treatment regimens for mitochondrial diseases including MELAS are designed to mitigate the cellular consequences of dysfunction of the respiratory chain by supplementation with electron acceptors and reactive oxygen species scavengers such as creatine, coenzyme Q10, α-lipoic acid, and vitamins (riboflavin, thiamine, vitamin C, vitamin E, and biotin); however, the clinical efficacy of these supplements remains limited or doubtful (Sproule and Kaufmann, 2008). Recently, pyruvate treatment was found to alleviate muscle impairment in patients with not only MELAS (Tanaka et al., 2007) but also other mitochondrial diseases such as Leigh's syndrome (Koga et al., 2012a; Komaki et al., 2010) and mitochondrial depletion syndrome (Saito et al., 2012) without causing notable side effects, and thus is considered promising as an alternative therapeutic. Metabolic mechanisms of pyruvate efficacy in MELAS mutant cells, however, are not clearly understood. We thus aimed to

* Corresponding author at: Department of Genomics for Longevity and Health, Tokyo Metropolitan Institute of Gerontology, 35-2 Sake-cho, Itabashi, Tokyo 173-0015, Japan. Tel.: +81 3 3964 3241x3095; fax: +81 3 3579 4776.
E-mail address: mtanaka@tmig.or.jp (M. Tanaka).
[1] These authors contributed equally to this work.

1567-7249/$ – see front matter © 2012 Elsevier B.V. and Mitochondria Research Society. All rights reserved.
http://dx.doi.org/10.1016/j.mito.2012.07.113

elucidate the metabolic responses of pyruvate-supplemented MELAS mutant cells by performing time-course metabolome analysis using capillary electrophoresis time-of-flight mass spectrometry or CE-TOFMS (Soga et al., 2003, 2006). Metabolomics technologies make it possible to simultaneously identify and quantify hundreds of metabolites contained in cells (Ishii et al., 2007; Ohashi et al., 2008), tissues (Hirayama et al., 2009; Soga et al., 2006) or body fluids (Soga et al., 2006; Sugimoto et al., 2010). Among other analysis platforms frequently used in metabolomics research, such as liquid chromatography or gas chromatography combined with mass spectrometry (LC-MS and GC-MS, respectively) and nuclear magnetic resonance (NMR) analysis, CE-TOFMS specializes in a comprehensive measurement of charged compounds (Soga et al., 2003) and thus is best suited to quantitatively analyze alterations of energy metabolism in cells. In addition, the use of ^{13}C-labeled compounds and quantification of the resulting ^{13}C-labeled isotopomers enable an investigator to trace small amounts of labeled compounds, thus facilitating our understanding of metabolic fluxes. Therefore, we used this approach to measure and quantify time-course changes in 161 intracellular metabolites in, and 85 metabolites released into the medium (hereafter referred to as medium metabolites) by, cybrid human 143B osteosarcoma cells containing normal mitochondria (2SA cells) or MELAS mutant mitochondria (2SD cells) cultured with 10 mM [3-^{13}C] pyruvate. Since most MELAS patients exhibit a symptom of lactic acidosis in addition to seizures and stroke-like events (*e.g.*, 94 of 101 (94%), 97 of 102 (96%), and 106 of 107 (99%) patients, respectively (Hirano and Pavlakis, 1994)), the medium was supplemented with 10 mM [3-^{13}C] lactate as a comparative control condition. The resulting metabolomic profiles highlighted the basal metabolic differences between 2SA and 2SD cells and their metabolic alterations and flux patterns in response to a high dose of lactate or pyruvate. In particular, constantly low ATP levels and poor energy charge characterized the basal metabolism of lactate-supplied 2SD cells and were likely due to impaired oxidative phosphorylation; however, pyruvate administration improved the lactate-to-pyruvate ratio ([Lac]/[Pyr]) and NADH-to-NAD$^+$ ratio ([NADH]/[NAD]) in 2SD cells, which enhanced glycolysis and replenished TCA cycle intermediates for maintaining the ATP at a level as high as that in 2SA cells. These results demonstrated a dramatic and favorable effect of pyruvate administration on the energy metabolism of 2SD cells, supporting the idea that balancing the [NADH]/[NAD] ratio is crucial for facilitating active glycolysis and replenishing TCA intermediates in MELAS mutant cells for a sufficient and stable energy production.

2. Materials and methods

2.1. Cell culture

The 2SA and 2SD cybrid cell lines carrying 100% wild-type and 94% A3243G mutant mtDNA, respectively, were established by fusion of mtDNA-deficient $\rho^0$206 cells generated from human 143B osteosarcoma cell line with enucleated myoblasts derived from a MELAS patient (Chomyn et al., 1992; Tanaka et al., 2002; Yoneda et al., 1994). The cells were cultured in high-glucose Dulbecco's modified Eagle's medium (DMEM) supplemented with 10% fetal bovine serum, 1 mM sodium pyruvate, and 0.4 mM uridine and maintained under 5% CO_2 at 37 °C. The experiments were initiated by replacing the medium with DMEM supplemented with 10% fetal bovine serum, 0.4 mM uridine, and 10-mM [3-^{13}C] lactate or 10-mM [3-^{13}C] pyruvate.

2.2. Metabolite extraction

Cell and medium samples were obtained 0, 1, 2, and 4 h after 10 mM [3-^{13}C] lactate or 10 mM [3-^{13}C] pyruvate administration. The sample medium was mixed with methanol containing 50 μM internal standards (3-aminopyrolidine, L-methionine sulfone, trimesate, 2-morpholinoethanesulfonic acid, and D-camphor-10-sulfonic acid), Milli-Q water, and $CHCl_3$ in the ratio of 1:4:2:5. The cells were washed twice with 5% mannitol solution and covered with methanol (1 ml) containing 25 μM internal standards for enzyme inactivation. The methanol and cell mixtures were collected and mixed with Milli-Q water and $CHCl_3$ in the ratio of 2:1:2. Both the medium and cell sample solutions were then centrifuged at 20,000 ×*g* for 15 min, and the aqueous layers were collected for centrifugal filtration through a 5-kDa-cutoff filter at 9,000 ×*g* for 2.5 h. The extracted metabolites were concentrated with a centrifugal concentrator (Tomy, Tokyo, Japan) and stored at −80 °C until analysis could be performed. The appropriate volume of Milli-Q water was added for the dissolution of the concentrated metabolites immediately before the sample injection into the CE-TOFMS.

2.3. Metabolome analysis

Concentrations of all the charged compounds were measured by CE-TOFMS using the methods developed by (Soga et al., 2006, 2003). Briefly, for analyzing cations (Soga et al., 2006), a fused silica capillary (50 μm i.d. × 100 cm total length) was used with 1 M formic acid as both the running and preconditioning buffer. Each sample (approximately 3 nl) was injected by applying a pressure of 50 mbar for 3 s and a continuous voltage of +30 kV. A solution of 5 mM ammonium acetate and 0.5 μM reserpine in 50% (v/v) methanol in water was used as the sheath liquid at a flow rate of 10 μl/min. For analyzing anions (Soga et al., 2006), a commercially available cationic capillary, SMILE(+) (Nacalai Tesque, Kyoto, Japan), was used with 50 mM ammonium acetate solution (pH 8.5) as the running buffer and 50 mM acetic acid (pH 3.4) as the preconditioning buffer. Each sample (approximately 30 nl) was injected by applying a pressure of 50 mbar for 30 s and a continuous voltage of −30 kV. For analyzing nucleotides and coenzyme A compounds (Soga et al., 2007), the fused silica capillary and 50 mM ammonium acetate (pH 7.5) were used. A voltage of −30 kV was applied to the inlet capillary, along with pressure of 50 mbar, to maintain the conductive liquid junction at the capillary outlet.

2.4. Metabolome data processing

The CE-TOFMS data were preprocessed by our proprietary software, MasterHands, which calculates accurate *m/z*, quantifies peak areas from the electropherogram, and aligns the peaks of multiple datasets. We quantified the concentrations of 161 intracellular and 85 medium metabolites including ^{13}C-labeled isotopomers involved in primary energy metabolism such as glycolysis, pentose phosphate pathway (PPP), tricarboxylic acid (TCA) cycle, urea cycle, and the metabolism of amino acids and nucleotides. The average amount of each metabolite per cell was evaluated based on the number of viable cells, which was counted at each sampling time by using a Countess Automated Cell Counter (Invitrogen, Carlsbad, California, US). For pyruvate, lactate, phosphoenolpyruvate, Gly, Ala, Ser, Asn, Asp, citrate, isocitrate, 2-oxoglutarate, succinate, fumarate, and malate, intracellular amounts and medium concentrations of their isotopomers were evaluated, taking into account the natural isotope abundance of C, H, and O atoms, according to the method of van Winden et al. (2002). Subsequently, *z*-values were evaluated for each compound on the basis of the average values of the time-course data and presented as a heat map in relation to the values determined at t = 0 followed by Euclidean distance-based hierarchical clustering using MeV (Saeed et al., 2003). The processed datasets were also comprehensively visualized on metabolic pathways constructed by using VANTED software (Junker et al., 2006).

3. Results

3.1. Heat map representation of time-series metabolome data from 2SA and 2SD cells

The concentrations of 161 intracellular and 85 medium metabolites including ^{13}C-labeled isotopomers were comprehensively mapped onto

metabolic pathways to enhance viewability (Supplementary Fig. 1A and B for the cell and medium metabolome data, respectively). Overall trends of the intracellular metabolomic changes in 2SA and 2SD cells were analyzed by Euclidean-distance-based hierarchical clustering analysis, and the results were presented as a heat map (Fig. 1), which highlighted the following intriguing features: First, the metabolomic profiles of lactate- and pyruvate-supplied 2SA cells were analogous to each other except for the changes in the metabolites in cluster 2 including glycolytic and PPP intermediates such as sedoheptulose 7-phosphate, dihydroxyacetone phosphate, ribulose 5-phosphate, and glucose 1-phosphate. Second, the metabolomic profiles of the lactate-supplied 2SA and 2SD cells were significantly different, particularly regarding the changes in metabolites in cluster 1, such as essential amino acids and those in cluster 3, such as ATP and 2-oxoglutarate, which showed nearly opposite trends. Third, the trends of the pyruvate-supplied 2SA and 2SD cells, however, significantly resembled each other except for the changes in only a few TCA cycle intermediates and amino acids. This resemblance was made even clearer from the results of the principal component analysis of the time-course metabolome data (Fig. 2A), which illustrates that the metabolomic profiles of lactate-supplied 2SD cells were located in the 3rd quadrant and thus deviated from the other profiles, whereas those of pyruvate-supplied 2SA and 2SD cells were aggregated mostly in the 4th quadrant. Pyruvate administration thus exhibited a dramatic effect on the energy metabolism of the MELAS mutant 2SD cells, redressing their overall metabolomic profile such that it resembled the profile of 2SA cells as a whole.

3.2. Energy status and metabolic parameters

The energy charge in the lactate-supplied 2SD cells decreased to 0.92 in 4 h from the initiation of the experiment but was otherwise maintained at ~0.96 under the other conditions (Fig. 2B). In these lactate-supplied 2SD cells, the levels of ATP and resulting total adenylates also dropped but ADP and AMP levels slightly increased (Fig. 2B), which characterizes a defective energy production in 2SD cells when cultured with a high dose of lactate. A low basal ATP level in 2SD cells was also identified in a previous study of ours (Fujita et al., 2007). Since no significant difference was observed in the reduced- to oxidized-glutathione ratio ([GSH]/[GSSG]) or in the NADPH-to-$NADP^+$ ratio ([NADPH]/[NADP]), the redox status of the 2SD cells appeared to be relatively well-maintained even under lactate-supplied condition (Fig. 2B). In contrast, [Lac]/[Pyr] and [NADH]/[NAD] ratios significantly increased only in the lactate-supplied 2SD cells (Fig. 2B), which implies an enhancement of lactic acidosis, NAD^+ shortage, and resulting stagnations of NAD^+-dependent reactions. Indeed, levels of fructose 1,6-bisphosphate and dihydroxyacetone phosphate, metabolites upstream of the glyceraldehyde 3-phosphate dehydrogenase reaction, which requires NAD^+ as a cofactor, significantly increased in level only in the lactate-supplied 2SD cells (Supplementary Fig. 1A). Glycolytic ATP production thus might have been stagnated due to the high [NADH]/[NAD] ratio. With pyruvate treatment, however, the 2SD cells retained [Lac]/[Pyr] and [NADH]/[NAD] ratios as low as those in 2SA cells (Fig. 2B). Taken together, these results indicate that the energy and redox statuses of 2SA cells were relatively robust in response to a high dose of either lactate or pyruvate whereas those of 2SD cells were vulnerable and susceptible to a high dose of lactate but were well-maintained and greatly approximated to those of 2SA cells as a result of pyruvate treatment, which facilitated efficient ATP production and improved the energy status by decreasing the [Lac]/[Pyr] ratio and maintaining the [NADH]/[NAD] ratio.

3.3. Isotopomer distribution and amino acid metabolism

The changes in lactate or pyruvate metabolism of 2SA and 2SD cells were interpreted by examining the distribution of isotopomers in the cells (Fig. 3) and medium (Supplementary Fig. 2), which were derived from the [3-^{13}C] lactate or [3-^{13}C] pyruvate used to supplement the medium. The initial intracellular lactate level in 2SD cells (at $t=0$) was more than twice as high as that in 2SA cells (47.9 and 21.2 fmol/cell, respectively; Fig. 3). The lactate level in 2SD cells abruptly dropped 1 h after the medium replacement but gradually increased afterwards under both lactate- and pyruvate-supplied conditions, whereas that in 2SA cells was almost constant and remained low. The percentage of ^{13}C-labeled lactate to the total lactate in pyruvate-supplied 2SD cells was ~35% and unexpectedly higher than under the other conditions (~25%), which indicates that the proportion of lactate production from the medium-derived [3-^{13}C] pyruvate increased in the pyruvate-supplied 2SD cells. Intracellular pyruvate, in contrast, significantly increased only under the pyruvate-supplied condition (8.7- and 13.2-fold in 4 h in 2SA and 2SD cells, respectively) but was remained low and almost constant in lactate-supplied conditions. Accordingly, the [Lac]/[Pyr] ratio in pyruvate-supplied 2SD cells was lowered not by the decrease in lactate but primarily by the significant increase in pyruvate, which thus boosted the flux from pyruvate to lactate and thereby balanced the [NADH]/[NAD] ratio. In addition, the significant increase in unlabeled pyruvate in pyruvate-supplied 2SD cells implies that pyruvate treatment enhanced not only the influx of pyruvate from the medium into the cells but also the pyruvate production from other routes such as glycolysis. Similar to the trend of the pyruvate level, 2-oxoglutarate, fumarate, and malate levels in 2SD cells were also significantly higher under pyruvate-supplied condition than under the lactate-supplied condition, as were the proportions of ^{13}C-labeled isotopomers. Pyruvate administration thus enhanced the replenishment of these TCA cycle intermediates, which were produced partly from [3-^{13}C] pyruvate (~37% and ~3% in 2SA and 2SD cells, respectively, for 2-oxoglutarate and ~40% and ~18% in 2SA and 2SD cells, respectively, for both fumarate and malate) and largely from other metabolites. Nevertheless, this finding does not necessarily imply that the TCA cycle activity of 2SD cells was enhanced by pyruvate treatment, since $^{13}C_2$-isotopomers of most TCA cycle-intermediates, which were supposedly produced from [3-^{13}C] pyruvate after the 2nd or more cycles of the TCA cycle, were quantifiable in 2SA cells but were largely below the detection limits in 2SD cells, probably due to the impaired oxidation of NADH by the respiratory chain in the 2SD cells. Intracellular and medium levels of Ala under the pyruvate-supplied condition were also higher than those under the lactate-supplied one, with a high proportion of $^{13}C_1$-labeled isotopomers in both cell lines (~51% and ~50% in 2SA and 2SD cells, respectively). The increase in the concentrations of both labeled and unlabeled medium Ala in the pyruvate-supplied 2SD cells (Supplementary Fig. 2) is of particular significance among other changes of medium amino acids (Supplementary Fig. 3). These data imply that pyruvate treatment enhanced conversion of [3-^{13}C] pyruvate to $^{13}C_1$-alanine coupled with the glutamate to 2-oxoglutarate conversion by alanine aminotransferase, which might have contributed to the increase in 2-oxoglutarate (Fig. 3) while excreting Ala into the medium as a byproduct, especially in the pyruvate-supplied 2SD cells. Pyruvate treatment appears also to have enhanced Asp production in both cell lines, but the basal level of Asp was higher in 2SA cells than in 2SD ones. Although the levels of both ^{13}C-labeled and unlabeled Asp isotopomers increased in both cell lines, the $^{13}C_2$-labeled Asp isotopomer, which would have been produced from $^{13}C_2$-labeled

Fig. 1. Metabolomic profiles of 2SA and 2SD cells supplemented with 10-mM lactate or 10-mM pyruvate for 161 intracellular metabolites and 85 metabolites in the medium. The metabolite names preceded by "(m)" indicate the medium levels of the corresponding metabolites and the others indicate the intracellular levels. The total concentration of ^{13}C-labeled and -unlabeled isotopomers was used for pyruvate, lactate, phosphoenolpyruvate, Gly, Ala, Ser, Asn, Asp, citrate, isocitrate, 2-oxoglutarate, succinate, fumarate, and malate. Features of the clusters 1–3 are explained in the text.

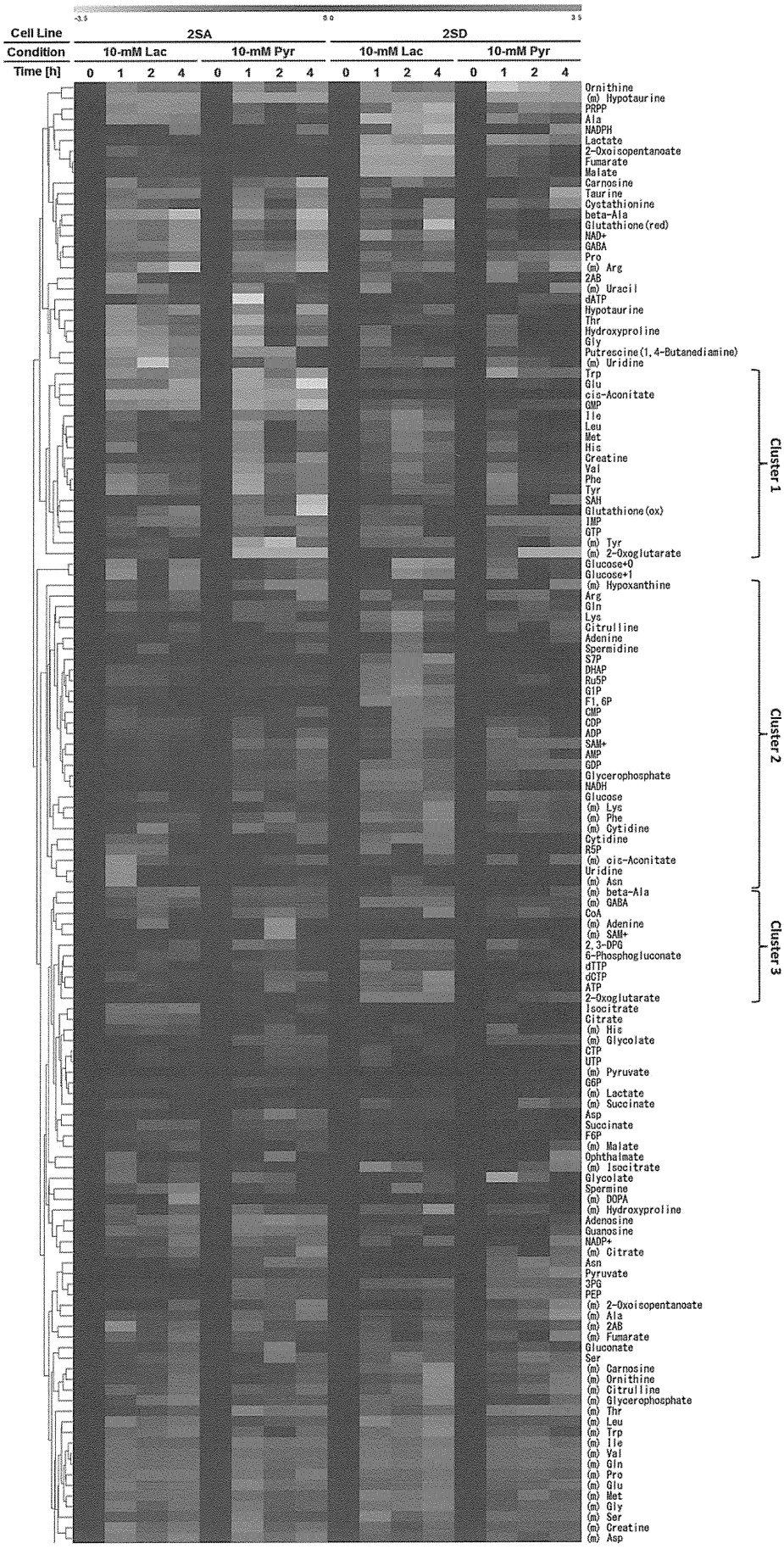
-3.5
0.0
3.5
Cell Line
2SA
2SD
Condition
10-mM Lac
10-mM Pyr
10-mM Lac
10-mM Pyr
Time [h]
0 1 2 4 0 1 2 4 0 1 2 4 0 1 2 4
Ornithine
(m) Hypotaurine
PRPP
Ala
NADPH
Lactate
2-Oxoisopentanoate
Fumarate
Malate
Carnosine
Taurine
Cystathionine
beta-Ala
Glutathione(red)
NAD+
GABA
Pro
(m) Arg
2AB
(m) Uracil
dATP
Hypotaurine
Thr
Hydroxyproline
Gly
Putrescine(1,4-Butanediamine)
(m) Uridine
Trp
Glu
cis-Aconitate
GMP
Ile
Leu
Met
His
Creatine
Val
Phe
Tyr
SAH
Glutathione(ox)
IMP
GTP
(m) Tyr
(m) 2-Oxoglutarate
Glucose+0
Glucose+1
(m) Hypoxanthine
Arg
Gln
Lys
Citrulline
Adenine
Spermidine
S7P
DHAP
Ru5P
G1P
F1,6P
CMP
CDP
ADP
SAM+
AMP
GDP
Glycerophosphate
NADH
Glucose
(m) Lys
(m) Phe
(m) Cytidine
Cytidine
R5P
(m) cis-Aconitate
Uridine
(m) Asn
(m) beta-Ala
(m) GABA
CoA
(m) Adenine
(m) SAM+
2,3-DPG
6-Phosphogluconate
dTTP
dCTP
ATP
2-Oxoglutarate
Isocitrate
Citrate
(m) His
(m) Glycolate
CTP
UTP
(m) Pyruvate
G6P
(m) Lactate
(m) Succinate
Asp
Succinate
F6P
(m) Malate
Ophthalmate
(m) Isocitrate
Glycolate
Spermine
(m) DOPA
(m) Hydroxyproline
Adenosine
Guanosine
NADP+
(m) Citrate
Asn
Pyruvate
3PG
PEP
(m) 2-Oxoisopentanoate
(m) Ala
(m) 2AB
(m) Fumarate
Gluconate
Ser
(m) Carnosine
(m) Ornithine
(m) Citrulline
(m) Glycerophosphate
(m) Thr
(m) Leu
(m) Trp
(m) Ile
(m) Val
(m) Gln
(m) Pro
(m) Glu
(m) Met
(m) Gly
(m) Ser
(m) Creatine
(m) Asp
Cluster 1
Cluster 2
Cluster 3

oxaloacetate, for example, was barely observed in 2SD cells, representing again their stagnated TCA cycle activity. Among other amino acids (Fig. 4 for cells and Supplementary Fig. 3 for medium), the Pro level was overall higher in 2SA cells than in 2SD cells. Despite our previous finding of the up-regulation of the asparagine synthetase (ASNS) gene in MELAS mutant cells through the elevation of ATF4 expression and its binding to NSRE-1 (Fujita et al., 2007), the change in the Asn level was not significantly different between cell lines but rather was dependent on lactate or pyruvate treatment in this study. Interestingly, the levels of all the essential amino acids except Thr were slightly but consistently higher in lactate-supplied 2SD cells than in those under the other conditions (Fig. 4), and this trend nevertheless disappeared by pyruvate treatment.

4. Discussion

MELAS syndrome is one of the most frequently occurring, maternally inherited mitochondrial disorders that devastatingly affect multiple organs including brain, nervous system, and muscles, as well as cognitive abilities. Although the efficacy of most treatment regimens has remained limited or doubtful (Sproule and Kaufmann, 2008), pyruvate was recently identified as an effective, safe, and affordable therapeutic agent that exhibits favorable effects on symptoms associated with not only MELAS (Tanaka et al., 2007) but also other mitochondrial diseases (Komaki et al., 2010; Saito et al., 2012). In order to elucidate the therapeutic mechanisms of pyruvate treatment from a viewpoint of energy metabolism, we used CE-TOFMS to investigate the metabolic profiles of the 2SA cells or MELAS mutant 2SD cells treated with 10 mM lactate or 10 mM pyruvate. The results revealed significant differences between the metabolomic profiles of 2SA and 2SD cells under the lactate-supplied condition and contrasting remarkable resemblances under the pyruvate-supplied condition. We previously reported that 2SD cells show up-regulated expression of genes associated with growth arrest (GADD45A, GADD45B, and CHOP) and exhibit a slower growth rate than their parental strain (Fujita et al., 2007). A recent study using human cybrid cells harboring the A3243G mutation also showed an increasing susceptibility of the cells to apoptosis and a high level of mutated mtDNA (Liu et al., 2004). Although no difference was observed between the cell viability of 2SA and 2SD cells in 4 h of culturing under the lactate- or pyruvate-supplied condition in this study (Supplementary Fig. 4), an unsound energy status of 2SD cells characterized by consistently low ATP levels and energy charges was observed under the lactate-supplied condition (Fig. 1), rationalizing their low cell viability in long-term cultures. Due to their limited capacity for oxidative phosphorylation-dependent ATP production, the lactate-supplied 2SD cells might have relied more on GTP and GTP → ATP conversion, which can be backed by relatively high GTP levels and significantly higher GTP-to-ATP ratios ([GTP]/[ATP]), than the cells in the other 3 groups (Supplementary Fig. 4). The increased IMP only in the lactate-supplied 2SD cells suggests a possibility of enhanced purine degradation via AMP deaminase. The energy metabolism of 2SD cells treated with lactate was thus not only defective in maintaining stable energy production but also unordinary in terms of their purine turnover.

The metabolomic profiles of the lactate-supplied 2SD cells exemplified the basal metabolism of MELAS patients with the symptom of lactic acidosis. With impaired mitochondrial complexes and a limited capacity for oxidative phosphorylation, 2SD cells are considered to rely inevitably on enhanced anaerobic glycolysis for ATP generation, which leads to increased flux from pyruvate to lactate and thus exacerbates lactic acidosis. ATP production via glycolysis is known to be stagnated when [Lac]/[Pyr] exceeds 25.6 (Voet and Voet, 1995). In both cell lines, the [Lac]/[Pyr] ratio was maintained below 25.6 under the pyruvate-supplied condition but not under the lactate-supplied one, under which the [Lac]/[Pyr] ratio in the normal 2SA cells was almost constant and ~43.1 but that in 2SD cells continuously increased and eventually exceeded 100 in 4 h. The 2SA cells can potentially shift their metabolism to oxidative phosphorylation for energy production when glycolysis is stagnated. In contrast, 2SD cells are left with ineffective glycolysis and intrinsically defective oxidative phosphorylation, and this situation impedes the production of sufficient ATP. Under the lactate-supplied condition, the increasing rate of the total (labeled and unlabeled) lactate concentration in the medium, which can be estimated by assuming a linear change in time and considering only the initial and final concentrations, was 731 and 919 fmol/cell/h in 2SA and 2SD cells, respectively, and that of unlabeled lactate in the medium was 765 and 1133 fmol/cell/h in 2SA and 2SD cells, respectively. Thus, the excretion rate of unlabeled lactate, which is probably the by-product of anaerobic glycolysis, appears to have been much higher in 2SD cells than in 2SA cells. Similarly, the decreasing rate (or incorporation rate into the cells) of $^{13}C_1$-labeled medium lactate was estimated and was again much higher in 2SD cells than in 2SA cells (206 and 32.6 fmol/cell/h, respectively), which thus shows a quick turnover of lactate in the lactate-supplied 2SD cells. Even under the pyruvate-supplied condition, the increasing rate of lactate (the total of labeled and unlabeled) was higher in 2SD cells than in 2SA cells (1310 and 676 fmol/cell/h, respectively). Unexpectedly, this increase in 2SD cells was even higher with pyruvate treatment in comparison with lactate treatment, indicating that pyruvate administration did not lower but rather enhanced lactate production. Although the trend of the total pyruvate concentration in the medium in 2SA and 2SD cells was analogous under the pyruvate-supplied condition, the turnover of medium pyruvate was also significantly higher in 2SD cells than in 2SA cells. The decreasing rate of $^{13}C_1$-labeled medium pyruvate was 353 and 536 fmol/cell/h in pyruvate-supplied 2SA and 2SD cells, respectively, while the increasing rate of unlabeled medium pyruvate was 271 and 424 fmol/cell/h in pyruvate-supplied 2SA and 2SD cells, respectively. Accordingly, pyruvate treatment significantly enhanced the incorporation of [3-^{13}C] pyruvate from and the excretion of lactate into the medium of 2SD cells, resulting in a balanced [NADH]/[NAD] and a sustainable ATP production primarily via anaerobic glycolysis in these cells. The [Lac]/[Pyr] ratio was therefore maintained low primarily by the alteration of pyruvate levels rather than lactate levels.

In lactate-supplied 2SD cells, the levels of essential amino acids increased (cluster 1 in Fig. 1), whereas 2-oxoglutarate and nucleoside triphosphates such as ATP, dTTP, and dCTP decreased (cluster 3 in Fig. 1); however, these characteristics were alleviated by pyruvate treatment, and the profile closely resembled that of the pyruvate-supplied 2SA cells. The differences in these metabolite profiles were rather trivial between lactate- and pyruvate-supplied 2SA cells. Supposedly, lactate was actively converted to pyruvate and then to TCA cycle intermediates for efficient oxidative phosphorylation in the 2SA cells, whereas lactate was hardly converted to pyruvate and rather accumulated in and out of the 2SD cells due to a high [NADH]/[NAD] ratio. In short, pyruvate treatment of 2SD cells facilitated their pyruvate-to-lactate conversion, decreased their [Lac]/[Pyr] ratio, and normalized their [NADH]/[NAD] ratio, and thus geared up their glycolysis for boosting ATP production and energy charge, without significantly changing the intracellular lactate level. This important finding implies that the decrease in lactate level is not necessarily essential to ameliorate the energy status of the MELAS mutant cells but rather that the lactate-to-pyruvate ratio and resulting [NADH]/[NAD] ratio are considered to be crucial. TCA cycle intermediates such as 2-oxoglutarate, fumarate, and malate significantly increased in level in the pyruvate-supplied 2SD cells. This increase might have been due to a potentially high activity of succinate dehydrogenase in 2SD cells, since a strong expression of succinate dehydrogenase in blood vessels is a well-known characteristic of MELAS patients (Hasegawa et al., 1991). The $^{13}C_1$-labeled isotopomers of these TCA cycle intermediates derived from ^{13}C-pyruvate accounted for ~2% of 2-oxoglutarate and ~17% of both fumarate and malate, and these proportions did not change considerably over a 4-h period; whereas the increase in unlabeled isotopomers contributed more to the increase in the total levels of these metabolites. Citrate and succinate, however, did not increase as much as the other TCA cycle intermediates in response to pyruvate treatment. These results imply that the addition of

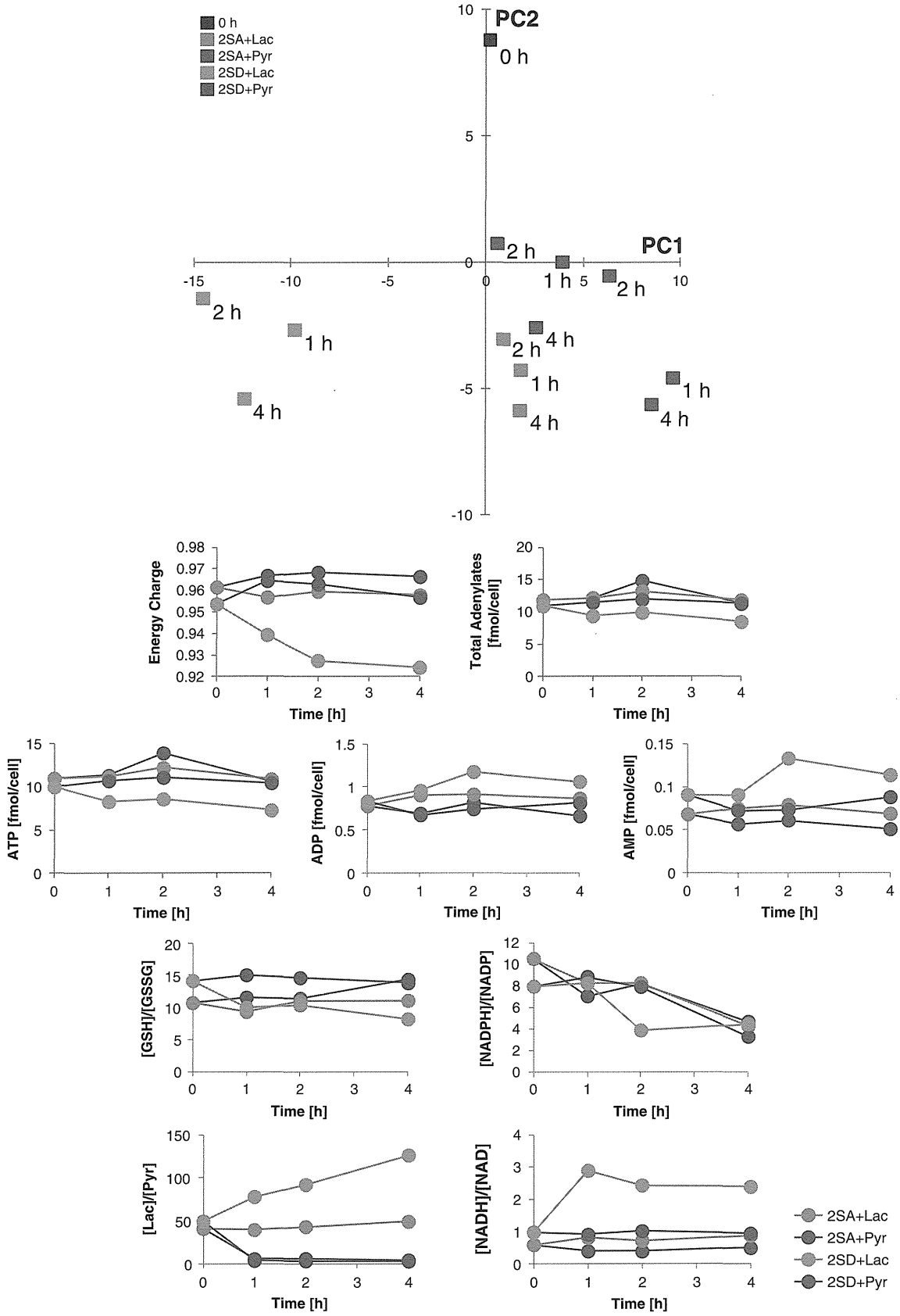

Fig. 2. A. Distributions of the principal component scores 1 (x-axis) and 2 (y-axis) of time-course metabolome data based on the intracellular and medium metabolites in 2SA and 2SD cells cultured with 10 mM lactate or 10 mM pyruvate. B. Time-course changes in metabolic parameters representing the energy status of 2SA and 2SD cells cultured with 10 mM lactate or 10 mM pyruvate. Energy charge was evaluated by ([ATP]+0.5×[ADP])/([ATP]+[ADP]+[AMP]); and total adenylates indicate the sum of ATP, ADP, and AMP levels.

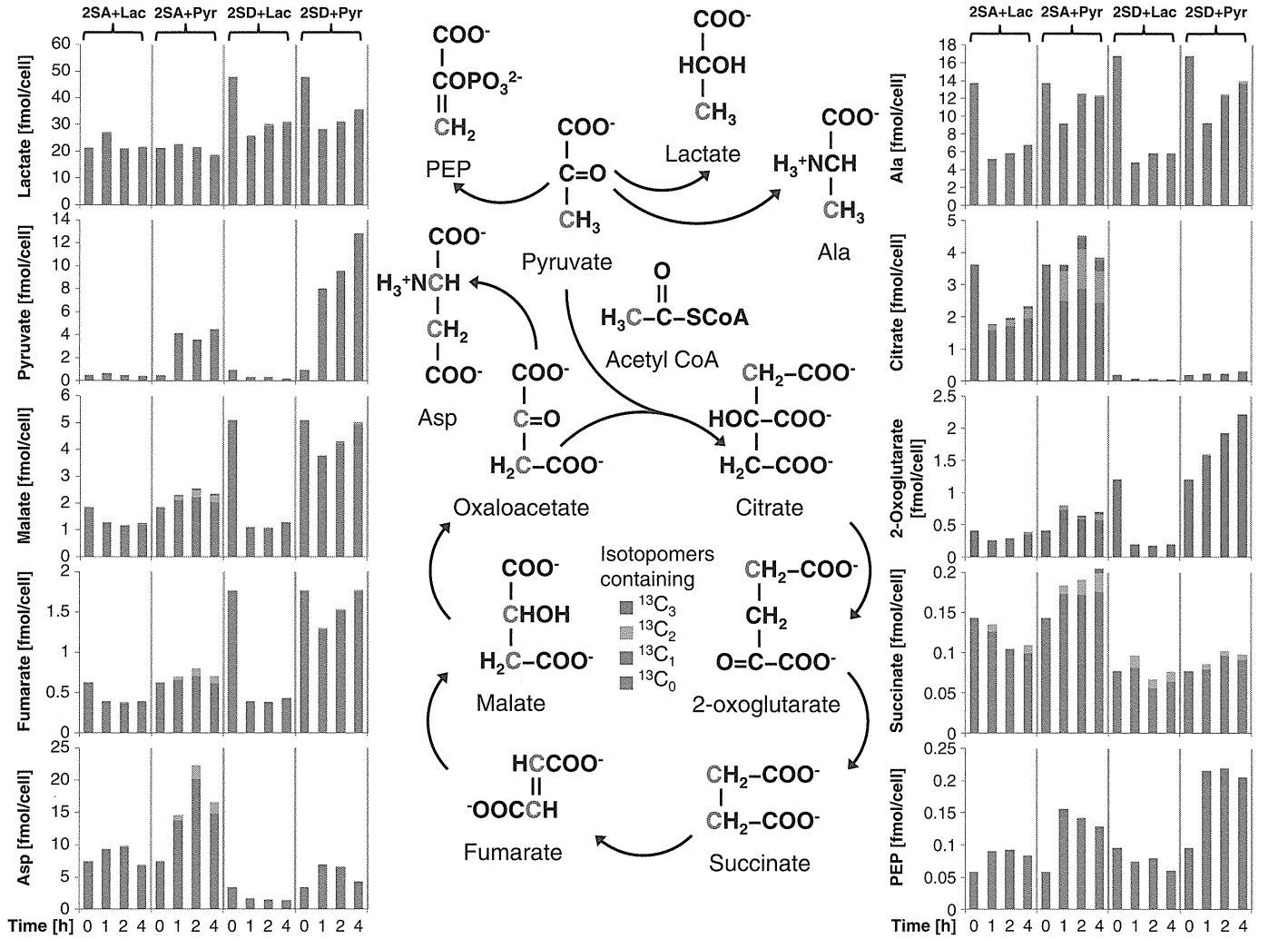

Fig. 3. Time-dependent changes in isotopomer proportions of intracellular pyruvate, lactate, PEP, Ala, Asp, and TCA cycle intermediates in 2SA and 2SD cells cultured with 10 mM lactate or 10 mM pyruvate. The colors of the bars represent the number of ^{13}C replaced with ^{12}C in the metabolites and isotopomers examined. The carbon atoms shown in black and red in each chemical structure represent the expected positions of ^{12}C and ^{13}C, respectively, in the first rotation of the TCA cycle. There are 2 possibilities considered for the ^{13}C position in succinate, fumarate, malate, oxaloacetate, and Asp.

pyruvate increased the metabolic flux not mainly from the pyruvate but from other sources to 2-oxoglutarate, fumarate, and malate. In this perspective, the balanced [NADH]/[NAD] ratio upon pyruvate treatment possibly enhanced the reactions involving NAD^+ as a cofactor. For example, the improved [NADH]/[NAD] ratio would have activated the glyceraldehyde 3-phosphate → 1,3-bisphosphoglycerate reaction by glyceraldehyde 3-phosphate dehydrogenase, which requires NAD^+ as a cofactor, and this would be the key for an optimal glycolytic ATP production in the pyruvate-supplied 2SD cells. In addition, the transaminase reaction involving the oxaloacetate + Glu → Asp + 2-oxoglutarate conversion might have been enhanced and contributed to the increased Asp and 2-oxoglutarate levels in the pyruvate-supplied 2SD cells. Since the malate dehydrogenase reaction also involves NAD^+, the significant increase in Asp, 2-oxoglutarate, fumarate, and malate levels in the pyruvate-supplied 2SD cells might have been due to the enhanced transamination cycle coupled with the urea cycle. Moreover, the glutamate → 2-oxoglutarate reaction by glutamate dehydrogenase and 2-oxoglutarate → succinyl-CoA reaction by 2-oxoglutarate dehydrogenase also require NAD^+ as a cofactor; thus, the activation of these reactions may have facilitated the succeeding succinyl CoA → succinate conversion for GTP production. This replenishment of TCA cycle intermediates and the balanced [NADH]/[NAD] ratio are considered essential for a limited but steady production of ATP via oxidative phosphorylation in 2SD cells, given that the expression of respiratory complexes I, III, and IV in 2SD cells is known to be decreased but not lost and that the expression of complex V is as high as that in their parental cells (Fujita et al., 2007). Although the pyruvate → acetyl CoA reaction by pyruvate dehydrogenase also involves NAD^+ as a cofactor, the pyruvate treatment did not significantly increase the intracellular citrate level. This result might have been due to a shortage of oxaloacetate, which combines with acetyl CoA for citrate production, or alternatively to a defect in pyruvate dehydrogenase and/or citrate synthase. In fact, pyruvate dehydrogenase deficiency and resulting altered oxidative phosphorylation function have been reported in a MELAS patient (Wilichowski et al., 1998), whereas citrate synthase activity in such a patient is reportedly nearly normal (Yoneda et al., 1989).

In the lactate-supplied 2SD cells, the levels of intracellular essential amino acids such as Ile, Leu, Met, His, Val, and Phe (cluster 1 in Fig. 1) and those of essential amino acids in the medium, such as Lys and Phe (cluster 2 in Fig. 1), accumulated significantly. The alteration of intracellular free amino acid pools in MELAS mutant cells was proposed based on our previous finding that ASNS gene expression is up-regulated in these cells (Fujita et al., 2007). MELAS mutant cybrids are known to exhibit autophagic cell death triggered by a combination of nitrosative and metabolic stress (Sandhu et al., 2005); thus, 2SD cells may have a constitutively high level of autophagic activity, and this might also have contributed to the generation of free amino acids by autophagic degradation of proteins and the resulting accumulation of essential

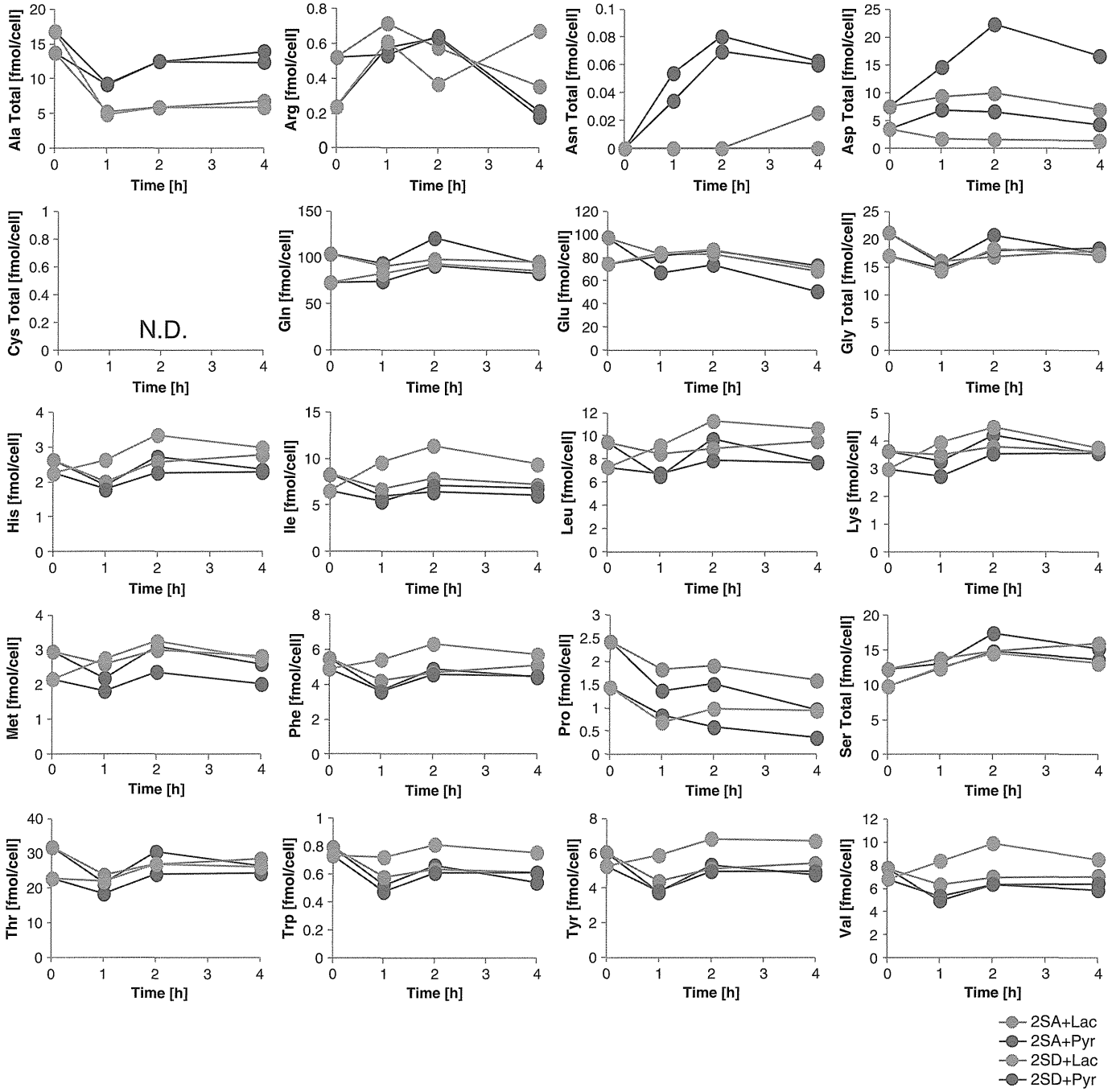

Fig. 4. Time-dependent changes in intracellular amino acid concentrations in 2SA and 2SD cells cultured with 10 mM lactate or 10 mM pyruvate. "N.D." indicates that the metabolite level was under the detection limit of CE-TOFMS analysis.

amino acids both intracellularly and in the medium. A high autophagic activity in 2SD cells can also be inferred by the increased production of reactive oxygen species (ROS) in MELAS syndrome (Rusanen et al., 2000), since ROS have been identified as signaling molecules to induce autophagy (Scherz-Shouval et al., 2007). In fact, the intracellular ROS level in 2SD cells is higher than that in 2SA cells (Fujita et al., 2007) and oxygen exposure-induced apoptosis is higher in MELAS mutant cells than in normal controls (Zhang et al., 1998). These findings thus imply that excessive ROS generated by the impaired respiratory chain facilitated autophagy in lactate-supplied 2SD cells, which eventually generated free amino acids and contributed to the increase in the levels of essential amino acids. In this perspective, the diminished accumulation of these essential amino acids in pyruvate-supplied 2SD cells may be explained by the fact that pyruvate is in fact a strong antioxidant and reacts with and reduces H_2O_2 (Desagher et al., 1997; Nath et al., 1995); thus, the pyruvate treatment might have alleviated oxidative stress and the accompanying autophagic activity in the 2SD cells.

Lactate is a well-known sensitive metabolic marker of MELAS (Castillo et al., 1995), which was also supported by its constantly high intracellular level and high increasing rate in the medium, as observed in this study. We also identified a few other metabolites that might function as potential MELAS markers. For example, the average increasing rate of medium Lys (Supplementary Fig. 3) in lactate-supplied 2SD cells (~171 fmol/cell/h) was significantly higher than that in the pyruvate-supplied 2SD cells (~53.7 fmol/cell/h) and 2SA cells (~33.8 fmol/cell/h under both lactate- and

pyruvate-supplied conditions). A possible reason for this high Lys level in the medium of the lactate-supplied 2SD cells might be the fact that the catabolism of Lys to acetyl CoA is known to involve 4 reactions that require NAD^+ as a cofactor; and thus this catabolic pathway may have been slowed down because of the constitutively low [NADH]/[NAD] ratio in the 2SD cells. Though to a lesser extent, a similar trend was observed in the increasing rate of Val in the medium (Supplementary Fig. 3; ~270 fmol/cell/h in lactate-supplied 2SD cells and ~202 fmol/cell/h under the other conditions). This may be again due to the shortage of NAD^+ in the lactate-supplied 2SD cells, as the catabolic pathway of Val to succinyl CoA is known to involve 3 reactions that require NAD^+ as a cofactor. The balanced [NADH]/[NAD] ratio seems critical also for the catabolism of these essential amino acids, since the increasing rate in these amino acids was lowered to the levels observed in 2SA cells by the pyruvate treatment. Although the overall trend of medium levels of Lys and Val appeared not to be considerably different among the conditions (Supplementary Fig. 3), this significant difference in the increasing rate of medium Lys and Val between the lactate-supplied 2SD cells and cells under the other conditions may be amplified in the long term. Accordingly, Lys and Val might be manifested in the blood or urine of MELAS patients and detectable as a diagnostic marker for MELAS and most likely other mitochondrial diseases showing imbalanced [NADH]/[NAD] as a pathologic condition. Moreover, gamma-aminobutyric acid (GABA) was one of the few metabolites that showed a clear cell line-specific trend independent of pyruvate- or lactate-administration (Supplementary Fig. 4). The intracellular GABA level in 2SA cells was nearly twice as high as that in 2SD cells throughout the experiment, and this trend was unchanged by either pyruvate or lactate treatment. Thus, GABA administration might be effective to somehow alleviate the symptoms of MELAS. Indeed, it has been speculated that treatment with inhibitory neurotransmitters such as GABA is theoretically effective to lower hyperexcitability in MELAS patients (Iizuka and Sakai, 2005).

Pyruvate administration does not always exhibit the expected efficacies in MELAS patients and not necessarily allow an optimistic outlook. This is perhaps by reason of the polygenetic nature of the cause of MELAS, which is known to be associated with at least 29 specific point mutations. There are at least 7 identified point mutations in the mitochondrial tRNA(Leu) gene, as well as mutations affecting many other mitochondrial tRNA genes (His, Lys, Gln, and Glu) and protein-coding genes (MT-ND1, MT-CO3, MT-ND4, MT-ND5, MT-ND6, and MT-CYB; (Sproule and Kaufmann, 2008)). Nevertheless, it is likely that the symptoms associated with lactic acidosis, *i.e.*, a high [NADH]/[NAD] ratio and possibly oxidative stress, would be alleviated by pyruvate administration. Current treatment regimens for MELAS patients involve indiscriminative administration of vitamins, cofactors, and oxygen-radical scavengers, which aims at the mitigation, postponement, or circumvention of the postulated damage to the respiratory chain (DiMauro and Schon, 2003). But pyruvate treatment could be a more effective, affordable, side effect-free, and most importantly, metabolically rational treatment regimen to improve symptoms associated with MELAS and even those of many other mitochondrial diseases. Such treatment would do so by facilitating efficient anaerobic glycolysis and probably supporting a limited but steady activity of oxidative phosphorylation for enhancing ATP production. Metabolome analysis of 2SA cells and MELAS mutant 2SD cells not only highlighted the basal metabolic differences between these cell lines but also their metabolic alterations and flux profiles in response to a high dose of lactate or pyruvate administration. The results showed a dramatic and sustainable effect of pyruvate administration on the energy metabolism of 2SD cells, supporting the idea that balancing the [NADH]/[NAD] ratio is crucial for facilitating anaerobic glycolysis for sufficient energy production in MELAS mutant cells. In this perspective, the efficacy of pyruvate treatment may not be limited to only alleviation of the symptoms associated with MELAS but rather also to that of those associated with a wider range of mitochondrial diseases.

Supplementary data to this article can be found online at http://dx.doi.org/10.1016/j.mito.2012.07.113.

Acknowledgments

The authors thank Dr. Masahiro Sugimoto for software development and Dr. Maria R. Monton and Ms. Kaori Igarashi for conducting the metabolome analysis. This work was supported in part by the following grants: a grant of the Global COE Program entitled, "Human Metabolomic Systems Biology," "Grant-in-Aid" research grants for the 21st Century Centre of Excellence (COE) Program (F-3); Scientific Research (A-22240072 and B-21390459), Creative Scientific Research (180 73004, 18GS0314), Targeted Proteins Research Program (TPRP), and Scientific Research on Priority Areas "Systems Genomes" and "Lifesurveyor" from the Ministry of Education, Culture, Sports, Science, and Technology (MEXT) of Japan; Grant-in-Aids (H23-016, H23-119, and H24-005) for the Research on Intractable Diseases (Mitochondrial Disease) from the Ministry of Health, Labour and Welfare (MHLW) of Japan; grants for scientific research from the Takeda Science Foundation; a grant for biological research from Gifu Prefecture, Japan; and research funds from the Government of Yamagata Prefecture and Tsuruoka City, Japan.

References

Castillo, M., Kwock, L., Green, C., 1995. MELAS syndrome: imaging and proton MR spectroscopic findings. AJNR Am. J. Neuroradiol. 16, 233–239.

Chomyn, A., Martinuzzi, A., Yoneda, M., Daga, A., Hurko, O., Johns, D., Lai, S.T., Nonaka, I., Angelini, C., Attardi, G., 1992. MELAS mutation in mtDNA binding site for transcription termination factor causes defects in protein synthesis and in respiration but no change in levels of upstream and downstream mature transcripts. Proc. Natl. Acad. Sci. U. S. A. 89, 4221–4225.

Desagher, S., Glowinski, J., Premont, J., 1997. Pyruvate protects neurons against hydrogen peroxide-induced toxicity. J. Neurosci. 17, 9060–9067.

DiMauro, S., Schon, E.A., 2003. Mitochondrial respiratory-chain diseases. N. Engl. J. Med. 348, 2656–2668.

Fujita, Y., Ito, M., Nozawa, Y., Yoneda, M., Oshida, Y., Tanaka, M., 2007. CHOP (C/EBP homologous protein) and ASNS (asparagine synthetase) induction in cybrid cells harboring MELAS and NARP mitochondrial DNA mutations. Mitochondrion 7, 80–88.

Goto, Y., Nonaka, I., Horai, S., 1990. A mutation in the tRNA(Leu)(UUR) gene associated with the MELAS subgroup of mitochondrial encephalomyopathies. Nature 348, 651–653.

Hasegawa, H., Matsuoka, T., Goto, Y., Nonaka, I., 1991. Strongly succinate dehydrogenase-reactive blood vessels in muscles from patients with mitochondrial myopathy, encephalopathy, lactic acidosis, and stroke-like episodes. Ann. Neurol. 29, 601–605.

Hirano, M., Pavlakis, S.G., 1994. Mitochondrial myopathy, encephalopathy, lactic acidosis, and strokelike episodes (MELAS): current concepts. J. Child Neurol. 9, 4–13.

Hirayama, A., Kami, K., Sugimoto, M., Sugawara, M., Toki, N., Onozuka, H., Kinoshita, T., Saito, N., Ochiai, A., Tomita, M., Esumi, H., Soga, T., 2009. Quantitative metabolome profiling of colon and stomach cancer microenvironment by capillary electrophoresis time-of-flight mass spectrometry. Cancer Res. 69, 4918–4925.

Hussein, A., Kasmani, R., Irani, F., Mohan, G., Ashmawy, A., 2009. An uncommon cause of lactic acidosis: MELAS. Eur. J. Intern. Med. 20, e114–e115.

Ichiki, T., Tanaka, M., Kobayashi, M., Sugiyama, N., Suzuki, H., Nishikimi, M., Ohnishi, T., Nonaka, I., Wada, Y., Ozawa, T., 1989. Disproportionate deficiency of iron-sulfur clusters and subunits of complex I in mitochondrial encephalomyopathy. Pediatr. Res. 25, 194–201.

Iizuka, T., Sakai, F., 2005. Pathogenesis of stroke-like episodes in MELAS: analysis of neurovascular cellular mechanisms. Curr. Neurovasc. Res. 2, 29–45.

Ishii, N., Nakahigashi, K., Baba, T., Robert, M., Soga, T., Kanai, A., Hirasawa, T., Naba, M., Hirai, K., Hoque, A., Ho, P.Y., Kakazu, Y., Sugawara, K., Igarashi, S., Harada, S., Masuda, T., Sugiyama, N., Togashi, T., Hasegawa, M., Takai, Y., Yugi, K., Arakawa, K., Iwata, N., Toya, Y., Nakayama, Y., Nishioka, T., Shimizu, K., Mori, H., Tomita, M., 2007. Multiple high-throughput analyses monitor the response of *E. coli* to perturbations. Science 316, 593–597.

Junker, B.H., Klukas, C., Schreiber, F., 2006. VANTED: a system for advanced data analysis and visualization in the context of biological networks. BMC Bioinforma. 7, 109.

Koga, Y., Povalko, N., Katayama, K., Kakimoto, N., Matsuishi, T., Naito, E., Tanaka, M., 2012a. Beneficial effect of pyruvate therapy on Leigh syndrome due to a novel mutation in PDH E1alpha gene. Brain Dev. 34, 87–91.

Koga, Y., Povalko, N., Nishioka, J., Katayama, K., Yatsuga, S., Matsuishi, T., 2012b. Molecular pathology of MELAS and l-arginine effects. Biochim. Biophys. Acta 1820, 608–614.

Komaki, H., Nishigaki, Y., Fuku, N., Hosoya, H., Murayama, K., Ohtake, A., Goto, Y., Wakamoto, H., Koga, Y., Tanaka, M., 2010. Pyruvate therapy for Leigh syndrome due to cytochrome c oxidase deficiency. Biochim. Biophys. Acta 1800, 313–315.

Liu, C.Y., Lee, C.F., Hong, C.H., Wei, Y.H., 2004. Mitochondrial DNA mutation and depletion increase the susceptibility of human cells to apoptosis. Ann. N. Y. Acad. Sci. 1011, 133–145.

Nath, K.A., Ngo, E.O., Hebbel, R.P., Croatt, A.J., Zhou, B., Nutter, L.M., 1995. alpha-Ketoacids scavenge H2O2 in vitro and in vivo and reduce menadione-induced DNA injury and cytotoxicity. Am. J. Physiol. 268, C227–C236.

Ohashi, Y., Hirayama, A., Ishikawa, T., Nakamura, S., Shimizu, K., Ueno, Y., Tomita, M., Soga, T., 2008. Depiction of metabolome changes in histidine-starved *Escherichia coli* by CE-TOFMS. Mol. Biosyst. 4, 135–147.

Pavlakis, S.G., Phillips, P.C., DiMauro, S., De Vivo, D.C., Rowland, L.P., 1984. Mitochondrial myopathy, encephalopathy, lactic acidosis, and strokelike episodes: a distinctive clinical syndrome. Ann. Neurol. 16, 481–488.

Rusanen, H., Majamaa, K., Hassinen, I.E., 2000. Increased activities of antioxidant enzymes and decreased ATP concentration in cultured myoblasts with the 3243A–>G mutation in mitochondrial DNA. Biochim. Biophys. Acta 1500, 10–16.

Saeed, A.I., Sharov, V., White, J., Li, J., Liang, W., Bhagabati, N., Braisted, J., Klapa, M., Currier, T., Thiagarajan, M., Sturn, A., Snuffin, M., Rezantsev, A., Popov, D., Ryltsov, A., Kostukovich, E., Borisovsky, I., Liu, Z., Vinsavich, A., Trush, V., Quackenbush, J., 2003. TM4: a free, open-source system for microarray data management and analysis. Biotechniques 34, 374–378.

Saito, K., Kimura, N., Oda, N., Shimomura, H., Kumada, T., Miyajima, T., Murayama, K., Tanaka, M., Fujii, T., 2012. Pyruvate therapy for mitochondrial DNA depletion syndrome. Biochim. Biophys. Acta 1820, 632–636.

Sandhu, J.K., Sodja, C., McRae, K., Li, Y., Rippstein, P., Wei, Y.H., Lach, B., Lee, F., Bucurescu, S., Harper, M.E., Sikorska, M., 2005. Effects of nitric oxide donors on cybrids harbouring the mitochondrial myopathy, encephalopathy, lactic acidosis and stroke-like episodes (MELAS) A3243G mitochondrial DNA mutation. Biochem. J. 391, 191–202.

Scherz-Shouval, R., Shvets, E., Fass, E., Shorer, H., Gil, L., Elazar, Z., 2007. Reactive oxygen species are essential for autophagy and specifically regulate the activity of Atg4. EMBO J. 26, 1749–1760.

Soga, T., Ohashi, Y., Ueno, Y., Naraoka, H., Tomita, M., Nishioka, T., 2003. Quantitative metabolome analysis using capillary electrophoresis mass spectrometry. J. Proteome Res. 2, 488–494.

Soga, T., Baran, R., Suematsu, M., Ueno, Y., Ikeda, S., Sakurakawa, T., Kakazu, Y., Ishikawa, T., Robert, M., Nishioka, T., Tomita, M., 2006. Differential metabolomics reveals ophthalmic acid as an oxidative stress biomarker indicating hepatic glutathione consumption. J. Biol. Chem. 281, 16768–16776.

Soga, T., Ishikawa, T., Igarashi, S., Sugawara, K., Kakazu, Y., Tomita, M., 2007. Analysis of nucleotides by pressure-assisted capillary electrophoresis-mass spectrometry using silanol mask technique. J. Chromatogr. A 1159, 125–133.

Sproule, D.M., Kaufmann, P., 2008. Mitochondrial encephalopathy, lactic acidosis, and strokelike episodes: basic concepts, clinical phenotype, and therapeutic management of MELAS syndrome. Ann. N. Y. Acad. Sci. 1142, 133–158.

Sugimoto, M., Wong, D.T., Hirayama, A., Soga, T., Tomita, M., 2010. Capillary electrophoresis mass spectrometry-based saliva metabolomics identified oral, breast and pancreatic cancer-specific profiles. Metabolomics 6, 78–95.

Tanaka, M., Borgeld, H.J., Zhang, J., Muramatsu, S., Gong, J.S., Yoneda, M., Maruyama, W., Naoi, M., Ibi, T., Sahashi, K., Shamoto, M., Fuku, N., Kurata, M., Yamada, Y., Nishizawa, K., Akao, Y., Ohishi, N., Miyabayashi, S., Umemoto, H., Muramatsu, T., Furukawa, K., Kikuchi, A., Nakano, I., Ozawa, K., Yagi, K., 2002. Gene therapy for mitochondrial disease by delivering restriction endonuclease SmaI into mitochondria. J. Biomed. Sci. 9, 534–541.

Tanaka, M., Nishigaki, Y., Fuku, N., Ibi, T., Sahashi, K., Koga, Y., 2007. Therapeutic potential of pyruvate therapy for mitochondrial diseases. Mitochondrion 7, 399–401.

van Winden, W.A., Wittmann, C., Heinzle, E., Heijnen, J.J., 2002. Correcting mass isotopomer distributions for naturally occurring isotopes. Biotechnol. Bioeng. 80, 477–479.

Voet, D., Voet, J.G., 1995. Biochemistry, Second ed. John Wiley & Sons, New York.

Wilichowski, E., Korenke, G.C., Ruitenbeek, W., De Meirleir, L., Hagendorff, A., Janssen, A.J., Lissens, W., Hanefeld, F., 1998. Pyruvate dehydrogenase complex deficiency and altered respiratory chain function in a patient with Kearns-Sayre/MELAS overlap syndrome and A3243G mtDNA mutation. J. Neurol. Sci. 157, 206–213.

Yoneda, M., Tanaka, M., Nishikimi, M., Suzuki, H., Tanaka, K., Nishizawa, M., Atsumi, T., Ohama, E., Horai, S., Ikuta, F., Miyatake, T., Ozawa, T., 1989. Pleiotropic molecular defects in energy-transducing complexes in mitochondrial encephalomyopathy (MELAS). J. Neurol. Sci. 92, 143–158.

Yoneda, M., Miyatake, T., Attardi, G., 1994. Complementation of mutant and wild-type human mitochondrial DNAs coexisting since the mutation event and lack of complementation of DNAs introduced separately into a cell within distinct organelles. Mol. Cell. Biol. 14, 2699–2712.

Zhang, J., Yoneda, M., Naruse, K., Borgeld, H.J., Gong, J.S., Obata, S., Tanaka, M., Yagi, K., 1998. Peroxide production and apoptosis in cultured cells carrying mtDNA mutation causing encephalomyopathy. Biochem. Mol. Biol. Int. 46, 71–79.

Mitochondrion 12 (2012) 617–622

Contents lists available at SciVerse ScienceDirect

Mitochondrion

journal homepage: www.elsevier.com/locate/mito

Heteroplasmic m.1624C>T mutation of the mitochondrial tRNA^{Val} gene in a proband and his mother with repeated consciousness disturbances

Yoko Sangatsuda [a,1], Masayuki Nakamura [a,1], Akiyuki Tomiyasu [a], Akiko Deguchi [a], Yasutaka Toyota [b], Yu-ichi Goto [c], Ichizo Nishino [d], Shu-ichi Ueno [b], Akira Sano [a,*]

[a] Department of Psychiatry, Kagoshima University Graduate School of Medical and Dental Sciences, 8-35-1 Sakuragaoka, Kagoshima 890-8520, Japan
[b] Department of Neuropsychiatry, Ehime University Graduate School of Medicine, Shitsukawa, Toon, Ehime 791-0295, Japan
[c] Department of Mental Retardation and Birth Defect Research, National Institute of Neuroscience, National Center of Neurology and Psychiatry, 4-1-1 Ogawahigashi, Kodaira, Tokyo 187-8502, Japan
[d] Department of Neuromuscular Research, National Institute of Neuroscience, National Center of Neurology and Psychiatry, 4-1-1 Ogawahigashi, Kodaira, Tokyo 187-8502, Japan

ARTICLE INFO

Article history:
Received 3 July 2012
Received in revised form 3 September 2012
Accepted 2 October 2012
Available online 10 October 2012

Keywords:
Mitochondrial DNA mutation
m.1624C>T
Mitochondrial tRNA^{Val} gene
Heteroplasmy
Neuropsychiatric symptoms

ABSTRACT

Homoplasmic m.1624C>T mutation of the mitochondrial tRNA^{Val} gene was previously demonstrated to cause fatal neonatal Leigh syndrome. Here, we report the clinical phenotypes of a Japanese male and his mother with heteroplasmic m.1624C>T mutation. The 36-year-old male presented with repeated episodes of consciousness disturbance since the age of 25, cognitive decline, and personality change. Cerebrospinal fluid levels of lactate and pyruvate were elevated. His mother showed similar symptoms and course. The mutation m.1624C>T was identified heteroplasmically in the proband's muscle and leukocytes and in the mother's leukocytes. The heteroplasmy load decreased with age.

1. Introduction

Point mutations in mitochondrial DNA (mtDNA) are responsible for a group of mitochondrial encephalomyopathies, maternally inherited disorders characterized by impaired energy production. Several hundred mtDNA mutations are reported in the Human Mitochondrial Genome Database (Brandon et al., 2005) as being associated with mitochondrial diseases. Each cell has 2–100 mitochondria and each mitochondrion contains 4–10 copies of the mtDNA. Heteroplasmy is the presence of both normal and mutant mtDNA at different levels within the same cell or tissue and is reported to be associated with the phenotypic variation within mitochondrial disease (DiMauro and Moraes, 1993).

Here we describe the clinical phenotypes observed in a Japanese mother–child pair harboring heteroplasmic m.1624C>T mutation. This mutation, which maps within the MTTV gene that encodes an mt-tRNA (valine), affects the dihydrouridine loop that is highly conserved across species from yeast to human (McFarland et al., 2002). McFarland et al. reported severe sibling cases with homoplasmic m.1624C>T mutation, which caused infantile and fatal Leigh syndrome-like symptoms. Cytochrome c oxidase (COX)-deficient fibers were present in the skeletal muscle of these cases. The pathogenicity of the m.1624C>T mutation was confirmed by the extremely low steady-state levels of mt-tRNA^{Val} observed in m.1624C>T mutant cell lines and the cardiac and skeletal muscle of the patients. However, until now, there has been no report of a patient with heteroplasmic m.1624C>T mutation.

2. Patients and methods

2.1. Case reports

2.1.1. Proband

The proband is a 36-year-old male (Fig. 1A; II-3), who is 170.5 cm tall and weighs 61 kg (normal body mass index of 21). He is the third of four children of non-consanguineous Japanese parents. He was normal at

Abbreviations: ARMS, amplification refractory mutation system; COX, cytochrome c oxidase; CSF, cerebrospinal fluid; CT, computed tomography; Ct, threshold cycle; EEG, electroencephalogram; mtDNA, mitochondrial DNA; PCR, polymerase chain reaction; RFLP, restriction fragment length polymorphism; VARS2, valyl-tRNA synthetase 2; WAIS, Wechsler Adult Intelligence Scale.

* Corresponding author at: Department of Psychiatry, Kagoshima University Graduate School of Medical and Dental Sciences, Kagoshima University, 8-35-1 Sakuragaoka, Kagoshima 890-8520, Japan. Tel.: +81 99 275 5346; fax: +81 99 265 7089.
E-mail addresses: yoko38@m2.kufm.kagoshima-u.ac.jp (Y. Sangatsuda), nakamu36@m.kufm.kagoshima-u.ac.jp (M. Nakamura), aki-tomy@m2.kufm.kagoshima-u.ac.jp (A. Tomiyasu), akiko48@m2.kufm.kagoshima-u.ac.jp (A. Deguchi), yatoyota@m.ehime-u.ac.jp (Y. Toyota), goto@ncnp.go.jp (Y. Goto), nishino@ncnp.go.jp (I. Nishino), ueno@m.ehime-u.ac.jp (S. Ueno), sano@m3.lufm.kagoshima-u.ac.jp, sano@m3.kufm.kagoshima-u.ac.jp (A. Sano).
[1] These authors contributed equally to this project and should be considered co-first authors.

1567-7249/$ – see front matter © 2012 Elsevier B.V. and Mitochondria Research Society. All rights reserved.
http://dx.doi.org/10.1016/j.mito.2012.10.002

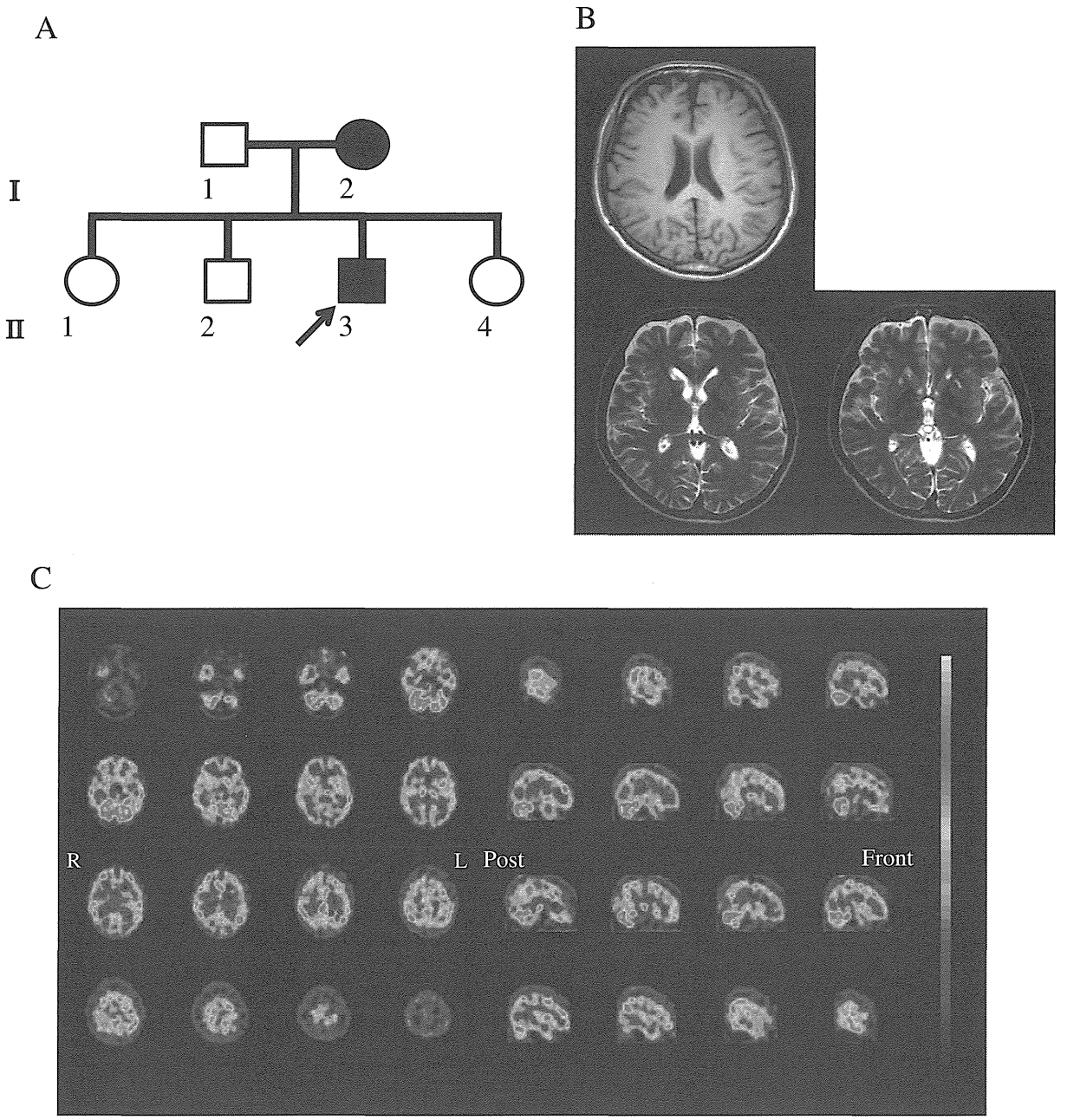

Fig. 1. Proband's family tree and brain imaging. (A) Pedigree of the family. The proband is indicated with an arrow. Affected and unaffected status is indicated by black and white symbols, respectively. (B) Brain magnetic resonance imaging of the proband revealed frontal lobe atrophy and high intensity on T2-weighted images and low intensity on T1-weighted images in the right caudate head and bilateral putamen. (C) Single photon emission computed tomography using technetium-99 m revealed reduction of cerebral blood flow in the proband's bilateral frontal lobe and the bilateral medial temporal lobe.

birth and grew well but dropped out of his high school. He then worked as a construction worker. His brother and sisters have neither neuromuscular nor neuropsychiatric symptoms. His personality gradually changed by age 36, developing irritability and emotional insecurity, which disrupted his relationships with others. He has been admitted to psychiatric hospital four times since he was 25 years old for repeated episodes of transient mild consciousness disturbance with delirious psychomotor agitation. These consciousness disturbances were not associated with lactic acidosis (data not shown). He presented with neuropsychiatric symptoms including disinhibition, cognitive decline, and personality change. He did not exhibit hallucination and delusion.

An electrocardiograph and echocardiogram at age 29 revealed left ventricular hypertrophy. Electromyograms of the right biceps and right rectus femoris showed normal findings. Deafness, diabetes, or ptosis were not observed. The concentrations of both lactate and pyruvate in the cerebrospinal fluid (CSF) at ages 25 and 29 were elevated, but those in the serum were not elevated at age 25 (Table 1). At age 29, the serum pyruvate level was elevated, but the lactate level was normal. Serum creatine kinase was transiently elevated at age 29. There were no abnormal findings on tests of liver and renal function and electrolyte levels. The levels of serum amino acids, urinary amino acids, and serum organic acids (except lactate and pyruvate) were within normal limits. He showed labile neurological signs (Table 2). Although his eye movements were normal at the age of 25, oculomotor disturbance and constriction of the visual fields appeared transiently at age 29. He showed a symmetrical tendon reflex and Babinski's signs were not observed at age 25. At age 29, increased left patellar tendon reflex and bilateral Babinski's signs

Table 1
The concentration of lactate and pyruvate.

	Age	Lactate (10–20 mg/dl)	Pyruvate (0.62–1.2 mg/dl)
CSF[a]	25	28↑	1.3↑
	29	36↑	1.3↑
Peripheral blood	25	9	0.7
	29	16	1.1↑
Gas analysis	25	18 (pH 7.42)	N/A

[a] CSF = cerebrospinal fluid.

were observed, but these were not observed at age 36. Ataxic gait, slurred speech, and poor coordination were evident at ages 29 and 36. Consciousness disturbance and psychomotor agitation were significantly improved by carbamazepine treatment. Electroencephalograms (EEGs) showed a continuous 7-Hz slow wave rhythm at age 25. The slow wave abnormal EEG was improved after treatment with carbamazepine. Medication withdrawal-related relapses were observed several times. Disinhibition, cognitive decline, and personality change remained after treatment.

Table 3 shows the results of the neuropsychological examinations. His intelligence quotient score measured using the Wechsler Adult Intelligence Scale (WAIS)—Revised (Wechsler, 1981) and the WAIS-III (Wechsler, 1997) decreased slightly from 69 (WAIS-R) to 61 (WAIS-III) from ages 29 to 36. Assessment of frontal lobe function by the Trail-Making Test (Corrigan and Hinkeldey, 1987), the modified Stroop test (Ichiba et al., 2007), the Wisconsin card-sorting test (Nelson, 1976), and the word fluency test (Borkowski et al., 1967) revealed progressive impairment of frontal lobe functions from age 29 to 35. Brain magnetic resonance imaging at ages 25 (data not shown) and 35 (Fig. 1B) revealed mild frontal lobe atrophy and low and high signal intensity spots on T1- and T2-weighted images, respectively, in the right caudate head and bilateral putamen. Single photon emission computed tomography using technetium-99 m at the age of 25 revealed reduced cerebral blood flow in the frontal lobe (Fig. 1C). Muscle histopathology revealed moderate variability in fiber size but neither ragged-red fibers nor COX-deficient fibers.

2.1.2. Proband's mother

The proband's mother (Fig. 1A; II-2) is 65 years old. She was the first of four children of non-consanguineous Japanese parents. She was normal at birth and grew well. She worked as an office worker and got married at the age of 24. Since age 37, she has experienced repeated stroke-like episodes with a partial seizure with secondary generalization and status. Brain computed tomography (CT) revealed small low-density areas in the right occipital and parietal lobes, both of which had disappeared after 15 days. She was repeatedly admitted to general hospitals. She was admitted to a psychiatric hospital at age 38, because of psychomotor excitation with auditory and visual hallucinations and persecutory delusions. She heard noisy sounds as auditory hallucinations and saw flowers, clowns, and a yellow mattress as visual hallucinations. Deafness, diabetes, or ptosis were not observed. Serum pyruvate and lactate levels were normal. There were no abnormal findings on tests of liver and renal function and electrolyte levels.

Table 2
Neurological signs of the proband.

Neurological signs	Age		
	25	29	36
Oculomotor disturbance	(−)	(+)	(−)
Constriction of visual fields transiently	(−)	(+)	(−)
Increased left patellar tendon reflex	(−)	(+)	(−)
Babinski's signs	(−)	(+)	(−)
Ataxic gait	(−)	(+)	(+)
Slurred speech	(−)	(+)	(+)
Poor coordination	(−)	(+)	(+)

Table 3
Neuropsychological examinations.

Neuropsychological tests	Age	
	29	36
	WAIS-R[a]	WAIS-III
VIQ	73	63
PIQ	69	65
FIQ	69	61
Trail Making Test		
Part A	73 s	69
Part B	265 s	267 abort
Modified Stroop test		
Read around	48 s (error 1/50)	43 s (error 1/50)
Color naming	90 s (error 5/50)	88 s (error 16/50)
WCST[b]		
CAT1	3	2
CAT2	5	3
Word fluency test		
Category	8.0	8.0
Initial phoneme	3.3	1.7

[a] WAIS-R = Wechsler Adult Intelligence Scale—Revised.
[b] WCST = Wisconsin card sorting test.

CSF measurements of cell count, pressure, and total protein and sugar were also unremarkable although the CSF levels of pyruvate and lactate were not measured. She presented with transient consciousness disturbance, psychotic symptoms including auditory and visual hallucinations and persecutory delusions, and cognitive impairment including alexia, agraphia, and acalculia. On the fourth day of the admission, EEG revealed poor alpha rhythms, an excess of fast background, and asymmetrical occasional appearance of a slow wave. Neurological examination showed symmetrical tendon reflex, no paralysis, and no Babinski's signs. An echocardiogram revealed left ventricular hypertrophy. Brain CT revealed small low-density areas in the right occipital and parietal lobes, both of which had disappeared after a month. The EEG abnormality, consciousness disturbance, and psychiatric symptoms improved after treatment with carbamazepine and haloperidol, although the alexia, agraphia, and acalculia remained. She developed left-side paresis at the age of 48. Brain CT revealed a fresh infarction in the right parieto-occipital region. The alexia, agraphia, and acalculia were persistent.

2.2. Neuropsychological examination

The proband was examined using the WAIS-R (Wechsler, 1981), WAIS-III (Wechsler, 1997), the Trail-Making Test (Corrigan and Hinkeldey, 1987), the modified Stroop test (Ichiba et al., 2007), the Wisconsin card sorting test (Nelson, 1976), and the word fluency test (Borkowski et al., 1967).

2.3. Genetic analysis

Total DNA was extracted using a standard protocol from muscle biopsy samples and leukocytes. Written informed consent was obtained from all subjects. The research protocol and consent form were approved by the Institutional Review Boards of Kagoshima University and Ehime University.

2.4. Mutation analysis

The entire 16,569 bp of mtDNA was amplified in 27 overlapping polymerase chain reaction (PCR) fragments. All primers were designed using the 'Primer 3 plus' web interface (http://www.bioinformatics.nl/cgi-bin/primer3plus/primer3plus.cgi). Annealing temperatures and times were determined according to the primer sequence and sequence abundance, respectively. Amplified products were purified using a QIAquick PCR purification kit (Qiagen, Hilden, Germany), labeled using a BigDye Terminator v3.1 Cycle Sequencing Kit (Applied Biosystems, Foster City, CA), and

directly sequenced on an ABI PRISM 3130 Avant Genetic Analyzer (Applied Biosystems) (Kato et al., 2011).

2.5. Quantification of mtDNA heteroplasmy

2.5.1. Primers for ARMS (Table 4)

To measure low proportions of mutant heteroplasmy, we designed mismatched primers for an amplification refractory mutation system (ARMS) assay (Newton et al., 1989). The 3′ end of the forward primer for the wild-type or mutated sequence was designed to amplify only the mutated or wild-type sequence, respectively (Bai and Wong, 2004; Genasetti et al., 2007). All primers were designed using the 'Primer 3 plus' web interface. Primer specificity was tested by gradient PCR to achieve the best yield and specificity at the most suitable annealing temperature, to design a real-time assay.

2.5.2. Quantitative real-time PCR

We measured the proportion of the m.1624C>T mtDNA mutation by real-time PCR using the THUNDERBIRD SYBR qPCR Mix (TOYOBO, Osaka, Japan). A range of 5 to 40 ng of total DNA in a volume of 20 μl was used. Nonspecific bands and primer dimers, which lead to inaccurate quantification by real-time PCR, were not observed.

Real-time PCR was performed with an ABI Prism 7300 (Applied Biosystems) and universal cycling conditions (2 min at 50 °C, 10 min at 95 °C, 40 cycles of 15 s at 95 °C, and 1 min at 60 °C). At least nine separate experiments were performed.

2.5.3. Preparation of DNA for assay calibration

We prepared calibration curves using known amounts of cloned plasmid DNA containing the wild-type or mutant sequence. A 712-bp PCR product generated using primers mtF1095 and mtR1787 (Table 4) was cloned into the pGEM-T vector (Promega, Madison, WI). One plasmid contained m.1624C (wild type) and the other contained m.1624T (mutant). Plasmid DNA was purified with a FastPlasmid Mini kit (Eppendorf, Hamburg, Germany) and a NucleoBond Xtra Midi Plus kit (Macherey-Nagel, Düren, Germany) according to the manufacturer's protocols. To obtain accurate calibration curves, the empty pGEM-T vector was diluted into the reaction solution and the plasmid clone was digested with the restriction enzyme SpeI. The copy numbers of the wild-type and mutant DNA sequence were calculated based on the size and molecular weight of the plasmid DNA. The molecular weight of 1 kb of double-stranded DNA (6.6×10^5 g/mol) and Avogadro's number were needed for the calculation. The optimal concentrations of wild-type and mutant plasmid DNA were determined by PCR with the optimal ARMS primer for real-time PCR. In this way, we decided to use approximately 10^6 copies of the plasmid.

2.5.4. Measurement of mutant heteroplasmy

The calibration curves for both the wild-type and mutant mtDNA were included in each run. The copy number of the target sequence in the sample was calculated from the threshold cycle (Ct) number and the calibration curve. The proportion of m.1624C>T mutation was calculated from the copy number of the wild-type and mutant sequences.

Table 4
Primers.

Primers	Nucleotide positions	Primer sequences
For insert PCR		
F1095	1095–1114	5′TAGCCCTAAACCTCAACAGT3′
R1787	1787–1806	5′ATTTTTCATCTTTCCCTTGC3′
For ARMS		
1624C (Wild type)	1601–1624	5′CCAGAGTGTAGCTTAACACAAAGC3′
1624T (Mutation)	1601–1624	5′CCAGAGTGTAGCTTAACACAAAGT3′
Mismatch primers		
1624CC (Wild type)	1601–1624	5′CCAGAGTGTAGCTTAACACAAACC3′
1624CT (Mutation)	1601–1624	5′CCAGAGTGTAGCTTAACACAAACT3′

Underlined nucleotide corresponds to the mismatched nucleotide.

3. Results

3.1. Sequencing of mtDNA

Given that the proband's symptoms suggested a mtDNA defect, we sequenced the entire mtDNA from the proband's leukocytes and muscle and from the proband's mother's leukocytes. We identified a heteroplasmic m.1624C>T mutation (Fig. 2).

3.2. Quantification of the m.1624C>T heteroplasmy with ARMS

We drew calibration curves by plotting the logarithm of the plasmid copy number against the Ct value. For the calibration plots, we used step-wise dilutions of an m.1624T mutant plasmid as the template for real-time PCR with the ARMS method (Fig. 2). For each sample mtDNA, we plotted the Ct number on the calibration curves; we were then able to calculate the proportion of the m.1624C>T mutation in the sample.

The proportions of the m.1624C>T mutation in the proband's muscle at age 29, muscle at age 36, leukocytes at age 29, leukocytes at age 36, in his mother's leukocytes, and in a control individual's leukocytes were 88.8%, 59.7%, 47.8%, 34.0%, 17.2%, and 0%, respectively (Fig. 2).

4. Discussion

Several reports have demonstrated the existence of mtDNA mutations in patients with psychiatric disorders such as depression, bipolar disorder, schizophrenia, mental retardation, and Asperger syndrome (Fattal et al., 2006; Kato et al., 2011; Munakata et al., 2007; Rollins et al., 2009; Rossignol and Frye, 2012). In the present study, we identified heteroplasmic m.1624C>T mutation in the proband and his mother, who both suffered from neuropsychiatric symptoms including repeated episodes of consciousness disturbance and psychomotor agitation with elevation of lactate and pyruvate in the CSF. This suggests that the neuropsychiatric symptoms are strongly associated with mitochondrial dysfunction in these patients.

Despite the m.1624C>T mutation being present in the proband's muscle at 88.8% at age 25 and 59.7% at age 36, no muscle pathology or mitochondrial myopathy were observed except for variability in fiber size. This is in contrast to a previous study, in which COX-deficient fibers were present in the muscles of individuals with homoplasmic m.1624C>T mutation (McFarland et al., 2002). Jeppesen et al. (2006) demonstrated that there was a clear threshold m.3243A>G mutation level at which morphological abnormalities, including COX-deficient fibers and ragged-red fibers, occurred. Similarly, there may be a threshold m.1624C>T mutation level at which pathological abnormalities occur in skeletal muscle. In the present study, neuropsychological tests in the proband showed slowly progressive cognitive decline with frontal lobe dysfunction. The presence of neuropsychiatric symptoms, imaging findings, and elevation of lactate and pyruvate in the absence of muscle symptoms and pathology indicate that the condition is more similar to mitochondrial encephalopathy than it is to mitochondrial encephalomyopathy.

The proportions of mitochondrial heteroplasmy have been calculated by real-time PCR or restriction fragment length polymorphism (RFLP) analysis. However, RFLP analysis may not be sufficiently sensitive to detect a low proportion of mutated mtDNA. Bai et al. described that the validity of real-time quantitative PCR using allele-specific TaqMan probes was similar to that of RFLP analysis because nonspecific binding of the mutant TaqMan probe to wild-type target DNA, and vice versa, disrupts quantitative analysis if there is a low proportion of

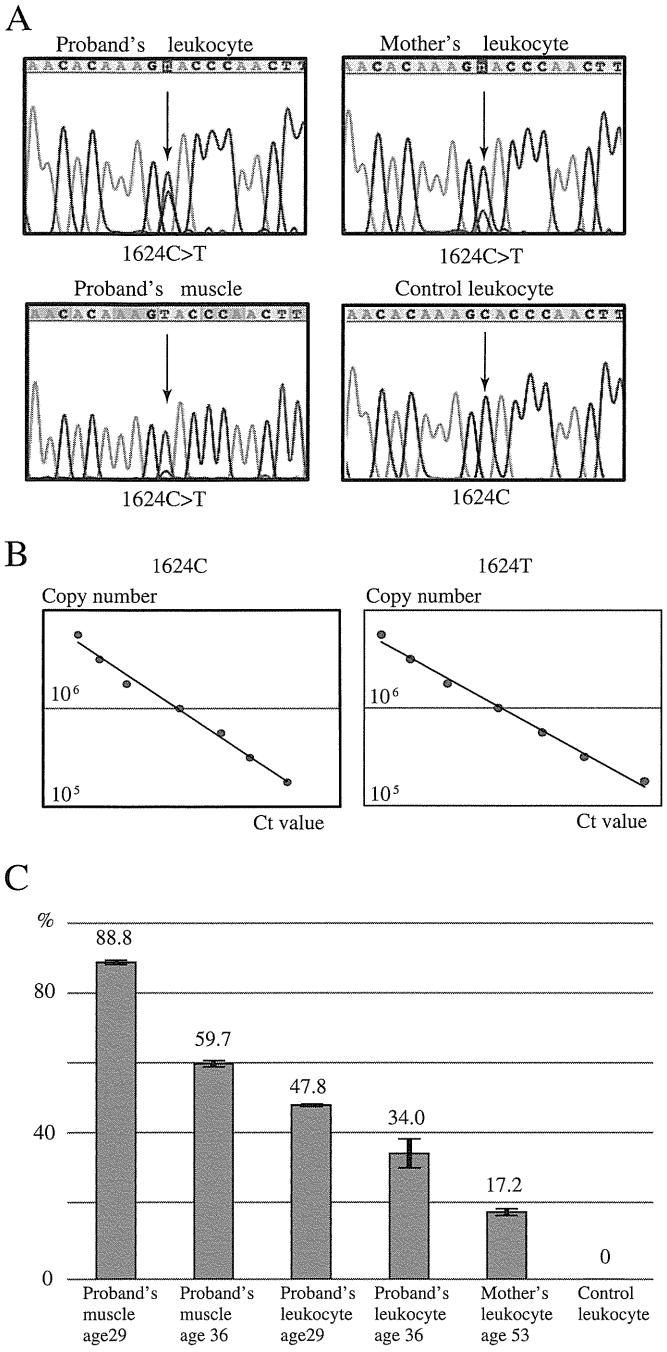

Fig. 2. Analysis of mtDNA. (A) Sequencing revealed m.1624C>T heteroplasmy in the proband's leukocytes and muscle and in the mother's leukocytes, but not in leukocytes from a control individual. The m.1624C>T mutation is indicated by arrows. In the mother's leukocytes, there is a low proportion of heteroplasmy, almost at the level of background noise. (B) Calibration curves of mutant mtDNA (m.1624T) and wild-type mtDNA (m.1624C). Step-wise dilutions of a plasmid containing the site of mutation were used as templates for real-time PCR with the ARMS method. Calibration curves were obtained by plotting the logarithm of the plasmid copy number against the Ct value. (C) Bar graph showing the proportions of the m.1624C>T mutation, calculated by plotting each Ct value on the calibration curves. The data are shown as mean ± SD ($n = 9$).

mutant mtDNA (Bai and Wong, 2004). These authors recommended the ARMS assay, which was developed to measure a low proportion of mutant heteroplasmy and is more accurate than using TaqMan probes in this situation. In the present study, we first detected heteroplasmy by mtDNA sequencing, although a low proportion of heteroplasmy can be masked in the background noise. As demonstrated in other studies (Bai and Wong, 2004; Genasetti et al., 2007; Sakiyama et al., 2011), using ARMS, we were able to detect variable proportions of the m.1624C>T mutation.

The proportion of heteroplasmic mtDNA is generally one determinant of phenotypic severity (Choi et al., 2010; Laloi-Michelin et al., 2009). Compared with the severely affected Leigh syndrome-like siblings with homoplasmic m.1624C>T mutation, our heteroplasmic cases showed milder phenotypes with respect to the age of onset and clinical features (Table 5); the lower proportion of mutant mtDNA might be responsible for this. However, the siblings' mother, who also harbored homoplasmic m.1624C>T mutation, suffered from comparatively milder symptoms, such as occasional migraine headaches, fatigue, and proximal muscle weakness (McFarland et al., 2002), implying that there may be additional modifying factors.

Rorbach et al. discussed how variations in the levels of VARS2 (called VARS2L in this paper) between tissue types and patients could underlie the difference in clinical presentation among individuals with homoplasmic m.1624C>T mutation (Rorbach et al., 2008). Our results agree that variable proportions of the m.1624C>T mutation, and consequently of VARS2, could cause differences in the clinical phenotype between individuals with m.1624C>T mutation.

We showed a reduction in the proportion of heteroplasmic m.1624C>T mutation in the proband's leukocytes and muscle over 7 years (Fig. 2). Similarly, previous reports (Olsson et al., 2001; 't Hart et al., 1996) have demonstrated that the proportion of heteroplasmic m.3243A>G mutation in leukocytes decreases with advancing age. This may be because of selection against high levels of pathogenic mtDNA in cells with rapid turnover (Olsson et al., 2001; 't Hart et al., 1996). Alternatively, another report revealed that, in diabetic patients, the somatic m.3243A>G mutation accumulated with age and the duration of diabetes (Nomiyama et al., 2004). In addition, the m.3243A>G mutation tends to accumulate and increase in abundance in post-mitotic cells with advancing age (Zhang et al., 1998). It is unknown why the load of m.1624C>T mutation in our proband's muscle reduced with age. A similar age-related decrease in m.13167A>G load with age (Zhang et al., 1998) was explained as follows: the mutation is generated during oocyte development or early embryogenesis, but the mutant molecules replicate more slowly than wild-type molecules do, leading to a decline in abundance with age. Post-mortem findings have indicated that the mutation load is similar among post-mitotic tissues (skeletal muscle, nervous system, and cochlea) (Macmillan et al., 1993; Shiraiwa et al., 1993). Thus, the proportion of m.1624C>T mutation, which is perhaps similar between muscle and brain, may be affected by slow

Table 5
Comparison of symptoms in the patients from this report and the patients studied by McFarland et al. (2002). qPCR analysis of heteroplasmy is provided for our family. The percentage of m.1624C>T heteroplasmy, onset of the ages and symptoms are given.

	Our patients		McFarland et al.'s (2002) patients	
	Proband	Mother	Mild case	Severe cases
Percentage of m.1624C>T heteroplasmy (%)				
Leukocyte	47.8 (age 29) 34.0 (age 36)	17.2 (age 53)	100 (age 35)	100 (infantile to <85 h after birth)
Muscle	88.8 (age 29) 59.7 (age 36)	NA[a]	100 (age 35)	100 (infantile to <85 h after birth)
Onset of age	25	38	<35	<0
Symptoms of onset	CD[b]	CD[b]	Unknown	Lethal or Leigh-symptoms

[a] NA = not available.
[b] CD = consciousness disturbance.